Lecture Notes on High Energy Astrophysics

Hsiang-Kuang Chang

Institute of Astronomy
National Tsing Hua University

Updated to the end of Chapter 2, 2026.01.26

Contents

Chapter 1

Introduction to High Energy Astrophysics

1.1 As a sub-field of astrophysics

This lecture is about high energy astrophysics. In astronomy and astrophysics, there are various sub-fields. These are named according to different classification schemes and conventions. One may talk about solar physics, planetary science, stellar astronomy, galactic astronomy, extragalactic astronomy, and cosmology. This is more or less classified according to subjects. One may go even more specifically, talking about subjects like helioseismology, asteroseismology, star and planet formation, interstellar medium, planetary nebulae, supernovae, compact stars, pulsars, X-ray binaries, black hole astrophysics, cosmic-ray astrophysics, galaxy evolution, active galaxies, galaxy clusters, high-redshift galaxies, large scale structure, and so on. There are too many to list.

One may also consider sub-fields based on physics contents involved, such as plasma astrophysics, relativistic astrophysics, high energy astrophysics, and particle astrophysics. Another way of classification is based on information carriers that are measured, such radio astronomy, infrared astronomy, optical astronomy, EUV astronomy, X-ray astronomy, gamma-ray astronomy, neutrino astronomy, and gravitational-wave astronomy.

Actually boundaries among different sub-fields are very often not well defined. High energy astrophysics is a sub-field that deals with systems

and phenomena involving high energy particles, usually referred to as being 'relativistic', and high energy emissions like X-rays and gamma rays. This 'lecture notes' covers mainly physical processes in high energy astrophysics, but not scientific subjects and observational technologies and facilities, which will be discussed in students classroom reports. Processes involving more details in plasma physics, general relativity, or nuclear and particle physics are not included either. Hopefully they can be covered in the future.

1.2 Subjects in high energy astrophysics

1.3 Instrumentation in high energy astrophysics

Chapter 2

Particle Acceleration

Energetic particles are observed or inferred to exist in many different systems and phenomena. They are seen in solar winds and cosmic rays. They are believed to be the cause of emissions from pulsars, pulsar wind nebulae, supernova remnants, astrophysical jets of different scales, and so on. Particles in cosmic rays of energy beyond 10^{20} eV have been observed. Their energy spectrum is often well described by power laws. It is clearly an interesting and intriguing question that how particles in the universe can get to such high energies.

To make particles more energetic, gravitational forces and electric forces are the two kinds of interaction in question. Acceleration by gravitational forces will be discussed in the next section. A large-scale, stable electric field is very rare in the universe because all the systems are of high electric conductivity and the field will be destroyed very quickly. The effect of electric acceleration, however, manifests itself in twofolds. One is electromagnetic, such as that in magnetic reconnection, plasma waves, and the potential drop developed by a fast rotating superconducting magnet like that in radio pulsars. The other is more dynamical, such as Fermi acceleration and shock acceleration, the ultimate working horse of which is electric fields. Acceleration in magnetic reconnection and plasma waves is more appropriate to discuss in plasma astrophysics. The development of electric fields in pulsar magnetospheres was originally proposed by Goldreich & Julian (1969). A rich research area of physics in pulsar magnetospheres has bloomed since then. One may refer to Becker (2009) for a collection of reviews on neutron stars and pulsars. We will discuss those dynamical ones, i.e. Fermi and shock

acceleration, in the sections after gravitational acceleration.

2.1   Acceleration by gravity

Particles gain kinetic energy when falling towards a mass due to gravity. Assuming zero velocity at infinity, a particle will have a speed

$$v = \sqrt{\frac{2GM}{r}} \tag{2.1}$$

when reaching at a distance r from the mass M, where G is the gravitational constant. For a central object of mass M and radius R, the highest speed a particle can get in this way depends on the compactness M/R.

For a white dwarf of mass $1M_\odot$ and radius 10^9 cm, that highest speed is about $v_{\max} \approx 5 \times 10^8$ cm/s. The corresponding Lorentz factor is $\gamma \approx 1.0002$. For a neutron star of mass $1M_\odot$ and radius 10^6 cm, we have $v_{\max} \approx 1.5 \times 10^{10}$ cm/s and $\gamma \approx 1.16$. Note that the $v_{\max}$ now is not negligible compared with c, so we may better consider a relativistic expression, that is,

$$(\gamma - 1)mc^2 = \frac{GMm}{R} \ , \tag{2.2}$$

from which we have $\gamma \approx 1.15$. However, because gravity is already quite strong in this case, the weak field approximation is no longer a good one. To go further, we will be in the realm of relativistic astrophysics. Nonetheless, the increase in the Lorentz factor that we see so far by gravity is still small, compared to cases with energies of TeV or beyond.

2.2   Fermi acceleration

Fermi proposed in 1949 a stochastic way for particle acceleration, in which particles collide with interstellar clouds randomly, or bounce back and forth between turbulent magnetic field irregularities in the interstellar medium. The key point is that particles gain more energy in head-on collisions than that lost in following collisions.

Consider the cloud to be infinitely massive and moving at velocity V, as shown in Figure 2.1. The particle is hitting the cloud with speed v at an

Figure 2.1: An infinitely massive cloud moves at speed V and a particle collides with it at angle θ.

angle θ. Its energy in the co-moving frame of the cloud is (recall the Lorentz transform)

$$E' = \gamma_V (E + V p \cos\theta) , \tag{2.3}$$

where $\gamma_V = \frac{1}{\sqrt{1-V^2/c^2}}$ and the x-component of the particle's momentum is $p_x = -p \cos\theta$. In this frame we also have

$$p'_x = -\gamma_V (p \cos\theta + \frac{V E}{c^2}) . \tag{2.4}$$

Assuming an elastic collision, E' is the same before and after the collision and p'_x changes its sign. Back to the observer's frame, we have the particle's energy to be

$$E'' = \gamma_V (E' + V(-p'_x)) . \tag{2.5}$$

Noting that $p/E = v/c^2$, the energy after one collision is

$$E'' = \gamma_V^2 E \left(1 + \frac{2 V v \cos\theta}{c^2} + (\frac{V}{c})^2 \right) . \tag{2.6}$$

Expanding this to second order in V/c, we find the energy change is

$$\triangle E = E'' - E = E\left(\frac{2Vv\cos\theta}{c^2} + 2(\frac{V}{c})^2\right) \; , \tag{2.7}$$

where one can see that particles gain more energy in head-on collisions than that lost in following collisions.

We now need to average over the angle θ. The probability of *hitting* at angle θ depends on two things. One is the relative speed of the approach of the particle and the cloud, that is, $v + V\cos\theta$. Note that the angle θ is the angle between the particle velocity and $-\vec{V}$. It is between 0 and $\pi/2$ for head-on collisions and between $\pi/2$ and π for following collisions. If we take $v \approx c$, this probability can be taken as proportional to $1 + (V/c)\cos\theta$. The other is the probability of being bewteen θ and $\theta + \mathrm{d}\theta$ is $\sin\theta\mathrm{d}\theta$. For the case of $v \approx c$, the average energy gain per collision is

$$\left\langle\frac{\triangle E}{E}\right\rangle = \frac{8}{3}\left(\frac{V}{c}\right)^2 \; , \tag{2.8}$$

which is second-order in V/c. *Note:* If the *hitting* probability is considered to be proportional to $|V + v\cos\theta| \propto |\frac{V}{c} + \cos\theta|$, instead of $v + V\cos\theta$, the above fractional energy gain will be $4\left(\frac{V}{c}\right)^2$. This probability consideration is more consistent with what we will discuss below for shock acceleration, but is different from that presented in Longair (2011). Fortunately this discrepancy does not affect our discussion below.

To see how such acceleration can result in a power-law distribution, let's consider the so-called diffusion-loss equation:

$$\frac{\partial n_E}{\partial t} = D\nabla^2 n_E + \frac{\partial(b\,n_E)}{\partial E} - \frac{n_E}{\tau} + Q \; , \tag{2.9}$$

where $n_E(E, \vec{r}, t)\mathrm{d}E\mathrm{d}^3x$ is the number of particles in $\mathrm{d}E\mathrm{d}^3x$ at a certain E and $\vec{r}$, D is the diffusion coefficient, b is the energy loss rate, $-\mathrm{d}E/\mathrm{d}t$, τ is the time scale for particles to remain in the acceleration region, and Q is the source term. The term containing b can be understood from the continuity equation in the energy space. Readers should always pay attention to positive and negative signs used in the text. For a steady-state solution without diffusion and sources, we have

$$\frac{\partial(b\,n_E)}{\partial E} = \frac{n_E}{\tau} \; . \tag{2.10}$$

8

To get the energy loss rate b, let's assume ℓ is the average distance between collisions and therefore ℓ/c is the time between collisions. From Eq.(2.8) we can have

$$b = -\frac{\langle \triangle E \rangle}{\langle \triangle t \rangle} = -\frac{8}{3} \left(\frac{V^2}{c\ell} \right) E = -\alpha E \; , \tag{2.11}$$

which gives us

$$-\alpha \frac{\partial (E \, n_E)}{\partial E} = \frac{n_E}{\tau} \; . \tag{2.12}$$

The equation now becomes

$$\frac{\partial n_E}{\partial E} = -\left(1 + \frac{1}{\alpha\tau} \right) \frac{n_E}{E} \; , \tag{2.13}$$

with the solution that

$$n_E \propto E^{-q} \; , \tag{2.14}$$

where $q = 1 + \frac{1}{\alpha\tau}$. This power law comes from the energy independence of α and τ, that is, the energy change rate is linearly proportional to energy and the probability of remaining in the acceleration region does not depend on energy. It does not depend on the actual form of α.

This Fermi mechanism is second order in V/c and the typical collison distance ℓ could be quite long. Taking $V \approx 3$ km/s and $\ell \approx 0.1$ pc, we have $\alpha \approx 10^{-16.5}$ sec^{-1} in the energy change rate equation $\mathrm{d}E/\mathrm{d}t = \alpha E$. That will give an e-folding time scale of about 1 Gyr. It is therefore not efficient.

2.3   Basics of shock acceleration

Another mechanism, which involves only head-on collisions, was proposed and developed in 1970s. It is called diffusive shock acceleration: particles are accelerated at the shock front. Shock waves form when perturbation in the medium travels supersonically, such as that in front of supersonic shells of supernova remnants in the interstellar medium. In this mechanism, a flux of high energy particles of speed already close to c is assumed to be present both in front of and behind the shock. These are the particles to be further accelerated to a very high energy. They diffuse back and forth through the

shock front. Because of scattering by magnetic irregularities and turbulent motions on either side of the shock, their velocity quickly become isotropic in the frame of the moving fluid on either side of the shock.

The fluid mass density behind a strong shock, ρ_2, is that $\rho_2/\rho_1 = (\gamma + 1)/(\gamma - 1)$, where ρ_1 is the density in front of the shock and γ is the ratio of specific heats, $c_{\mathrm{p}}/c_{\mathrm{v}}$, of the fluid, if it is assumed to be a perfect gas (Landau & Lifshitz 1987, Chapter IX). Taking $\gamma = 5/3$ for monatomic gases, we have $\rho_2/\rho_1 = 4$. In the co-moving frame of the shock front, the upstream gas passes through the front with speed $v_1 = U$, where U is the shock wave speed in the medium. The downstream gas therefore, by the continuity of ρv, leaves the front with $v_2 = v_1/4$, that is, when observed in the laboratory frame, it moves at a speed of $\frac{3}{4}U$; see Figure 2.2.

Figure 2.2: A shock wave moving at speed U. The black solid line in the middle represents the shock front. To the right is the upstream region. To the left, the downstream region, gas moves at speed $\frac{3}{4}U$. High energy particles are assumed to be present in the fluid on either side of the shock. Their velocity distributions are isotropic in the rest frames of the upstream and downstream gases respectively.

Now consider the high energy particles in front of the shock (i.e., in the upstream region). They are isotropic in the frame of the upstream gas. The

shock moves at a speed U, but the gas behind the shock (i.e., in the downstream region) moves at $V = \frac{3}{4}U$, relative to the upstream gas. When some of those high energy particles pass through the shock, they will gain some energy from collision with dowmstream gas because that is basically all head-on ones. They will again become isotropic in the frame of the downstream gas, in which the uptream gas is also approaching at a speed of $\frac{3}{4}U$. And then, when those particles pass through the front, back to the upstream region, *they will again gain more or less the same fractional amount of energy.*

The energy E' in the downstream gas frame of a particle of energy E in the upstream (laboratory) frame is

$$E' = \gamma_V(E + Vp\cos\theta) , \qquad (2.15)$$

where the angle θ is defined in the same way as that in the Fermi mechanism. The strong shock is assumed to be non-relativistic, i.e., $U \ll c$, and therefore $V \ll c$ and $\gamma_V = 1$. Because particles are assumed to be already relativistic, i.e., $E = pc$, we have

$$\frac{\triangle E}{E} = \frac{E' - E}{E} = \frac{V}{c}\cos\theta . \qquad (2.16)$$

We do not bother to transform this energy back to the upstream-gas frame, because that will give a similar amount of energy gain, as shown below:

$$
\begin{aligned}
E'' &= \gamma_V(E' + Vp\cos\theta') \\
&= \gamma_V(\gamma_V(E + Vp\cos\theta) + Vp\cos\theta'). \\
&= \gamma_V E(\gamma_V + (\gamma_V\cos\theta + \cos\theta')\frac{V}{c}) \\
&\approx E(1 + (\cos\theta + \cos\theta')\frac{V}{c}) ,
\end{aligned}
$$

where in the last approximation γ_V is taken as unity.

The probability of particles *passing through the shock* at angle θ is proportional to their velocity component normal to the shock, $c\cos\theta$, and $\sin\theta d\theta$. Therefore, the average gain is

$$\left\langle \frac{\triangle E}{E} \right\rangle = \frac{V}{c}\frac{\int_0^{\pi/2}\cos^2\theta\sin\theta d\theta}{\int_0^{\pi/2}\cos\theta\sin\theta d\theta} = \frac{2}{3}\frac{V}{c} . \qquad (2.17)$$

After a round trip back to the upstream region, the fractional energy increase is, because of $V/c << 1$,

$$\left\langle \frac{\triangle E}{E} \right\rangle = \frac{4}{3}\frac{V}{c} \ . \tag{2.18}$$

Now we take a detour to obtain, in a somewhat different but similar way as in the last section, the power-law distribution of the accelerated particles. Consider a constant β so that $E = \beta E_0$ is the average energy of the particle after one single trip of the acceleration and another constant P for the probability for the particle to remain in the acceleration region after that trip. Then, after k trips, the particle number is $N = N_0 P^k$ and their energy is $E = E_0 \beta^k$. We therefore have

$$\frac{\ln(N/N_0)}{\ln(E/E_0)} = \frac{\ln P}{\ln \beta} \ , \tag{2.19}$$

that is,

$$\frac{N}{N_0} = \left(\frac{E}{E_0} \right)^{\ln P/\ln \beta} \ . \tag{2.20}$$

We may consider in a differential range $\mathrm{d}k$ of k there are $\mathrm{d}N = N_E(E)\mathrm{d}E$ and from the variation of the above equation we have

$$N_E(E)\mathrm{d}E \propto E^{-1+\ln P/\ln \beta}\mathrm{d}E \ . \tag{2.21}$$

Here, $N_E(E)$ corresponds to the n_E in Eq.(2.14). It is clear that $(\ln P/\ln \beta)$ is equal to $-\frac{1}{\alpha\tau}$ in Eq.(2.14), β is related to α, and P to τ.

For the survival probability P, we note that the number flux of high energy particles passing through the shock from upstream to downstream is $\int_{\theta=0}^{\frac{\pi}{2}} \frac{nc}{4\pi} \sin\theta\mathrm{d}\theta\mathrm{d}\phi \cos\theta = \frac{1}{4}nc$, where n is the number density at the shock. It is the number density of the high energy particles, which is not to be confused with that of the shocked fluid and is roughly constant everywhere near the shock. The quantity $\frac{nc}{4\pi}$ is the number flux per solid angle. The factor $\frac{1}{4}$ comes from the consideration of a unit area at the shock front, originating from the factor $\cos\theta$. In the downstream region there is a flow out of the shock at a speed of $\frac{1}{4}U$. We therefore expect a fractional flux of $(\frac{1}{4}nc - \frac{1}{4}nU)/(\frac{1}{4}nc)$

12

to come back. So we have $P = 1 - \frac{U}{c}$. For the shock acceleration we have $\ln P = \ln(1 - \frac{U}{c}) \approx -\frac{U}{c}$ and $\ln \beta = \ln(1 + \frac{4V}{3c}) \approx \frac{4V}{3c} = \frac{U}{c}$. And then we reach

$$N_E(E)\mathrm{d}E \propto E^{-2}\mathrm{d}E , \qquad (2.22)$$

whose power index is close to what is observed in many systems.

Sound speed in the interstellar medium is usually of order 10 km/s. Most interstellar clouds moves subsonically. In Fermi acceleration, $(V/c)^2$ is usually smaller than 10^{-8}. On the other hand, supernova remnant shells may move at about 10^4 km/s and therefore form strong shocks in the interstellar medium. The ratio U/c could be larger than 10^{-2}. Shock fronts are very thin, in particular compared with distance between interstellar clouds. Shock acceleration is thus much more efficient than Fermi acceleration. We note that so far we have considered only a non-relativistic strong shock, i.e., $c \gg U \gg c_\mathrm{s}$, where c is the speed of light and c_s the sound speed. A more complicated shock, such as those involving nonlinear or relativistic effects, or with the presence of strong magnetic fields, may further enhance the acceleration. A useful review can be found in Blandford & Eichler (1987).

Chapter 3

Bremsstrahlung

In this and the next chapters we will describe emissions from high-energy charged particles. When they emit photons in the Coulomb field of an ion, the emission is called bremsstrahlung. When they do so in a magnetic field, the emission is called synchrotron radiation. High-energy charges can also produce high-energy photons by scattering photons in a photon field. This kind of scattering, or emission, is called inverse Compton scattering. Scattering, however, will be treated together with other processes that occur between photons and matter when they encounter each other. It therefore also includes absorption and pair production, which will be discussed in later chapters. The properties of these processes can be obtained by QED calculations. Semi-classical approaches of derivation can be found in many textbooks, such as Rybicki & Lightman (1979). We will mainly describe their properties and this 'lecture notes' may serve as something like a reference book or manual for readers to easily find the needed formulae.

3.1 Bremsstrahlung of a single electron

We first consider one single electron passing through the Coulomb field of an ion of charge Ze with speed v at infinity and an impact parameter b. The bremsstrahlung spectrum for such an encounter is

$$\frac{\mathrm{d}E}{\mathrm{d}\omega}(\omega, v, b) = \begin{cases} \frac{8}{3}\frac{Z^2 e^6}{\pi c^3 m_{\mathrm{e}}^2 b^2 v^2} \ , & \text{for } \omega \ll \dfrac{\gamma v}{b} \\[2ex] 0 \ , & \text{for } \omega \gg \dfrac{\gamma v}{b} \end{cases} \tag{3.1}$$

(Jackson (1975), p.722; Longair (2011), p.165), where ω is the angular frequency of the emission and γ is the Lorentz factor of the electron.

For a single-speed population of electrons of number density n_e and speed v, the emissivity at frequency ω in a population of ions of charge Ze and number density n_i is

$$
\begin{aligned}
\frac{\mathrm{d}E}{\mathrm{d}\omega\,\mathrm{d}V\,\mathrm{d}t} &= \int_{b_\mathrm{min}}^{b_\mathrm{max}} n_\mathrm{e} v\, 2\pi b\, \mathrm{d}b\, \frac{\mathrm{d}E}{\mathrm{d}\omega}\, n_\mathrm{i} \\
&= \frac{16}{3}\frac{Z^2 e^6 n_\mathrm{e} n_\mathrm{i}}{c^3 m_\mathrm{e}^2 v}\ln\left(\frac{b_\mathrm{max}}{b_\mathrm{min}}\right)
\end{aligned}
\tag{3.2}
$$

The dependence on ω is weak (in the logarithm) and this is good only approximately up to ω_max, where $\hbar\omega_\mathrm{max} = \frac{1}{2}m_\mathrm{e}v^2$. The determination of b_min and b_max is not trivial. See the following for the result of a more accurate QM calculation.

The emissivity for given n_i, n_e, v, and ω is

$$
\frac{\mathrm{d}E}{\mathrm{d}\omega\,\mathrm{d}V\,\mathrm{d}t} = \frac{16}{3}\frac{\pi}{\sqrt{3}}\frac{Z^2 e^6 n_\mathrm{e} n_\mathrm{i}}{c^3 m_\mathrm{e}^2 v} g_\mathrm{ff}(v,\omega)\ ,
\tag{3.3}
$$

where

$$
g_\mathrm{ff}(v,\omega) = \frac{\sqrt{3}}{\pi}\ln\Lambda
\tag{3.4}
$$

is the Gaunt factor of bremsstrahlung, and

$$
\begin{aligned}
\ln\Lambda &= \ln\left(\frac{v_\mathrm{i} + v_\mathrm{f}}{v_\mathrm{i} - v_\mathrm{f}}\right) \\
&= \ln\left(\frac{1 + \sqrt{1 - \frac{\hbar\omega}{\frac{1}{2}mv_\mathrm{i}^2}}}{1 - \sqrt{1 - \frac{\hbar\omega}{\frac{1}{2}mv_\mathrm{i}^2}}}\right)\ ,
\end{aligned}
\tag{3.5}
$$

where we have used $\frac{1}{2}mv_\mathrm{i}^2 = \frac{1}{2}mv_\mathrm{f}^2 + \hbar\omega$. (Longair (2011), p.167; Chiu (1968), p.223). We note that although the Gaunt factor goes to infinity at $\omega = 0$ (Figure 3.1), its integration over ω gives a finite result.

The energy loss rate of electrons is then

$$
\begin{aligned}
\frac{\mathrm{d}E}{\mathrm{d}t} &= \frac{1}{n_\mathrm{e}}\int_{\hbar\omega=0}^{\hbar\omega=\frac{1}{2}mv^2} \frac{\mathrm{d}E}{\mathrm{d}\omega\,\mathrm{d}V\,\mathrm{d}t}\mathrm{d}\omega \\
&\propto n_\mathrm{i} Z^2 v \\
&\propto E^{\frac{1}{2}}\ ,
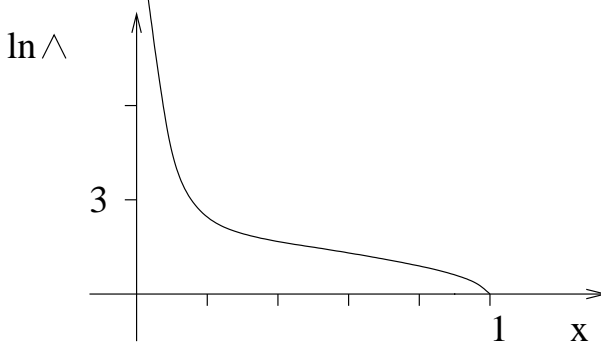\end{aligned}
\tag{3.6}
$$

15

Figure 3.1: $\ln \Lambda$ in the bremsstrahlung gaunt factor. The X-axis is $x = \hbar\omega / \frac{1}{2}mv_{\mathrm{i}}^2$.

where we have taken the Gaunt factor to be roughly constant. For ultra-relativistic cases, a similar result for $\mathrm{d}E/\mathrm{d}\omega\mathrm{d}V\mathrm{d}t$ can be found (Rybicki & Lightman (1979), Eq.(5.24); Longair (2011), Eq.(6.71)). Since $v \sim c$ and $\hbar\omega_{\mathrm{max}} \sim E$, we have approximately

$$\frac{\mathrm{d}E}{\mathrm{d}t} \propto E \tag{3.7}$$

(Longair (2011), p.175). All the above are for mono-energetic electrons. In general and in practice electrons usually have an energy spectrum.

3.2 Thermal bremsstrahlung

In thermal equilibrium, electrons follow the Maxwellian distribution:

$$\mathrm{d}P \propto v^2 \exp(-\frac{mv^2}{2kT})\mathrm{d}v \quad . \tag{3.8}$$

The emissivity that we discussed in the last section is then

$$\frac{\mathrm{d}E(T,\omega)}{\mathrm{d}\omega\,\mathrm{d}V\,\mathrm{d}t} = \frac{\int_{v_{\mathrm{min}}}^{\infty} \frac{\mathrm{d}E(v,\omega)}{\mathrm{d}\omega\,\mathrm{d}V\,\mathrm{d}t}\, v^2 \exp(-\frac{mv^2}{2kT})\mathrm{d}v}{\int_0^{\infty} v^2 \exp(-\frac{mv^2}{2kT})\mathrm{d}v} \quad . \tag{3.9}$$

Note that since $\frac{1}{2}mv^2 \geq \hbar\omega$, we have $v_{\mathrm{min}} = \sqrt{2\hbar\omega/m}$.

After integration, we have the thermal bremsstrahlung emissivity $\varepsilon_\nu^{\text{ff}} = \frac{\mathrm{d}E(T,\nu)}{\mathrm{d}\nu\,\mathrm{d}V\,\mathrm{d}t}$ as

$$
\begin{aligned}
\varepsilon_\nu^{\text{ff}} &= \frac{32\pi e^6}{3m_{\text{e}}c^3}\sqrt{\frac{2\pi}{3km_{\text{e}}}}Z^2 n_{\text{e}}n_{\text{i}}T^{-\frac{1}{2}}\exp(-\frac{h\nu}{kT})\bar{g}_{\text{ff}}(T,\nu) \\
&= 6.8\times10^{-38}Z^2 n_{\text{e}}n_{\text{i}}T^{-\frac{1}{2}}\exp(-\frac{h\nu}{kT})\bar{g}_{\text{ff}}(T,\nu) \quad\quad (3.10)
\end{aligned}
$$

in gaussian units. The velocity-averaged Gaunt factor, $\bar{g}_{\text{ff}}(T,\nu)$, is of order of unity ($5 > \bar{g}_{\text{ff}}(T,\nu) > 1$ for $10^{-4} < \frac{h\nu}{kT} < 1$). In the emissivity, the factor $T^{-\frac{1}{2}}$ comes from the $1/v$ dependence in the single electron emissivity, and the factor $\exp(-\frac{h\nu}{kT})$ comes from v_{min}. The (optically thin) thermal
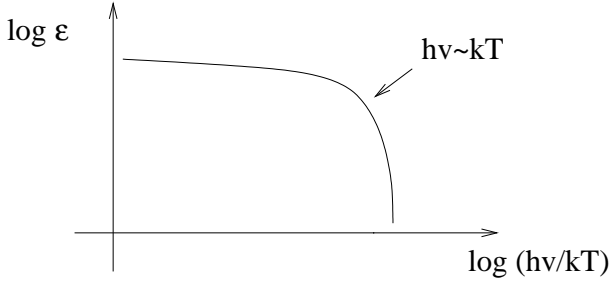

Figure 3.2: An optically-thin thermal bremsstrahlung spectrum

bremsstrahlung spectrum is quite flat until $h\nu \sim kT$.

The total power per unit volume is

$$
\begin{aligned}
\varepsilon^{\text{ff}} &= \int \varepsilon_\nu^{\text{ff}}\mathrm{d}\nu \\
&= \left(\frac{2\pi k}{3m}\right)^{\frac{1}{2}}\frac{32\pi e^6}{3hmc^3}Z^2 n_{\text{e}}n_{\text{i}}T^{\frac{1}{2}}\bar{g}_{\text{B}}(T) \\
&= 1.4\times10^{-27}Z^2 n_{\text{e}}n_{\text{i}}T^{\frac{1}{2}}\bar{g}_{\text{B}}(T) \quad\quad (3.11)
\end{aligned}
$$

in gaussian units. $\bar{g}_{\text{B}}(T)$ is the frequency average of $\bar{g}_{\text{ff}}(T,\nu)$. Its numerical value is between 1.1 and 1.5, so taking 1.2 should be good enough. For higher temperatures, relativistic corrections can be found as

$$
\varepsilon_{\text{rel}}^{\text{ff}} = \varepsilon^{\text{ff}}(1 + 4.4\times10^{-10}T) \quad\quad (3.12)
$$

17

(Rybicki (1979), p.165).

For thermal bremsstrahlung absorption, let's consider in a thermal plasma in which only bremsstrahlung occurs. From Kirchhoff's law, we have

$$\frac{j_\nu^{\rm ff}}{\alpha_\nu^{\rm ff}} = B_\nu(T) = \frac{2\nu^2}{c^2} \frac{h\nu}{\exp(\frac{h\nu}{kT}) - 1} \ . \tag{3.13}$$

Noting that $j_\nu^{\rm ff} = \frac{\varepsilon_\nu^{\rm ff}}{4\pi}$, we get

$$
\begin{aligned}
\alpha_\nu^{\rm ff} &= \frac{j_\nu^{\rm ff}}{B_\nu} \\
&= \frac{4}{3}\frac{e^6}{mch}\sqrt{\frac{2\pi}{3km}}Z^2 n_{\rm e} n_{\rm i} T^{-\frac{1}{2}}\nu^{-3}(1 - \exp(-\frac{h\nu}{kT}))\bar{g}_{\rm ff}(T,\nu) \\
&= 3.7 \times 10^8 Z^2 n_{\rm e} n_{\rm i} T^{-\frac{1}{2}}\nu^{-3}(1 - \exp(-\frac{h\nu}{kT}))\bar{g}_{\rm ff}(T,\nu) \tag{3.14}
\end{aligned}
$$

in gaussian units. We can see that absorption is strong for low frequencies. The corresponding opacity is therefore large for those frequencies and the plasma becomes optically thick. The thermal bremsstrahlung spectrum will behave as ν^2 like the Planck function at low frequencies and then turn into an optically thin thermal bremsstrahlung spectrum at higher frequencies.
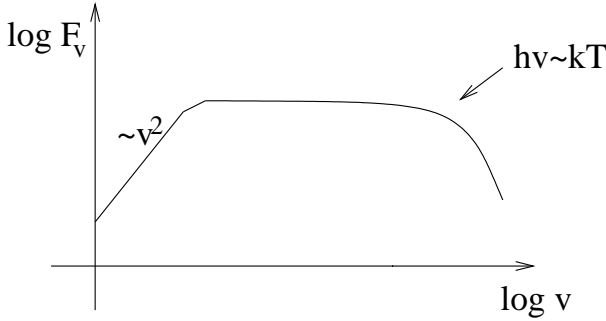

Figure 3.3: A broad-band thermal bremsstrahlung spectrum. Turning points in the spectrum may provide information about density and temperature of the emitting plasma.

With the factor of ν^{-3}, the Rosseland mean absorption coefficient is approximately like

$$\alpha_{\rm R}^{\rm ff} \propto T^{-\frac{7}{2}}Z^2 n_{\rm e} n_{\rm i} \bar{g}_{\rm ff,R}(T) \tag{3.15}$$

18

Noting that $\alpha = n\sigma = \rho\kappa$, we have

$$\kappa_{\mathrm{R}}^{\mathrm{ff}} \propto \rho T^{-\frac{7}{2}} \ , \tag{3.16}$$

which is called the Kramer opacity. The Rosseland mean opacity is extensively used in stellar astrophysics.

Chapter 4

Synchrotron and Curvature Radiation

4.1 Synchrotron and curvature radiation of a single electron

Emission of charged particles in a magnetic field has three names. The **cyclotron** radiation is referred to that of non-relativistic charges circulating (or spiraling) in a magnetic field and the **synchrotron** radiation is that for relativistic charges. The **curvature** radiation is the radiation of charges moving *along* curved magnetic field lines in their lowest Landau level.

The motion of a charged particle in a magnetic field.

The equation of motion reads

$$\frac{\mathrm{d}\gamma m\vec{v}}{\mathrm{d}t} = \frac{q}{c}\vec{v} \times \vec{B} \ . \tag{4.1}$$

Since the Lorentz force is always perpedicular to the velocity, if radiation loss is ignored, the energy of the particle remains constant, i.e., $\frac{\mathrm{d}\gamma}{\mathrm{d}t} = 0$. Therefore,

$$\gamma m \frac{\mathrm{d}\vec{v}}{\mathrm{d}t} = \frac{q}{c}\vec{v} \times \vec{B} \ , \tag{4.2}$$

which in turn gives

$$\frac{\mathrm{d}\vec{v}_\parallel}{\mathrm{d}t} = 0 \; , \tag{4.3}$$

and

$$\gamma m \frac{\mathrm{d}\vec{v}_\perp}{\mathrm{d}t} = \frac{q}{c}\vec{v}_\perp \times \vec{B} \; . \tag{4.4}$$

The gyrofrequency and the cyclotron frequency.

The motion of a charged particle in a magnetic field can therefore be decomposed into a motion parallel to the field direction and a gyromotion around the field. The angular frequecny of this gyromotion is

$$\omega_\mathrm{g} = \frac{qB}{\gamma mc} \; , \tag{4.5}$$

which we call the gyration frequency, or gyrofrequency. The gyroradius r_g is then

$$r_\mathrm{g} = \frac{v_\perp}{\omega_\mathrm{g}} = \frac{\gamma mvc\sin\alpha}{qB} = \frac{pc}{q}\frac{\sin\alpha}{B} \; , \tag{4.6}$$

where α is the pitch angle, i.e., the angle between $\vec{v}$ and $\vec{B}$, and $\frac{pc}{q}$ is sometimes called the rigidity. We distinguish the terminology of the gyrofrequency and the cyclotron frequency by defining the latter as

$$\omega_0 = \frac{qB}{mc} \; . \tag{4.7}$$

In Rybicki & Lightman (1979) the gyrofrequency is denoted as ω_B, while in some literatures ω_B, or sometimes ω_c, is used to refer to the cyclotron frequency. To avoid this notation confusion, we use ω_g and ω_0 in this lecture notes.

The curvature radius and the characteristic frequency.

Consider an arc path of a charged particle's motion as shown in Figure 4.1. What we want to find is the reciprocal of the time interval of an observed light pulse, expressed in terms of the particle energy and the curvature radius or the magnetic field strength. From Figure 4.1, we have $\Delta\theta \sim \frac{2}{\gamma}$ from the
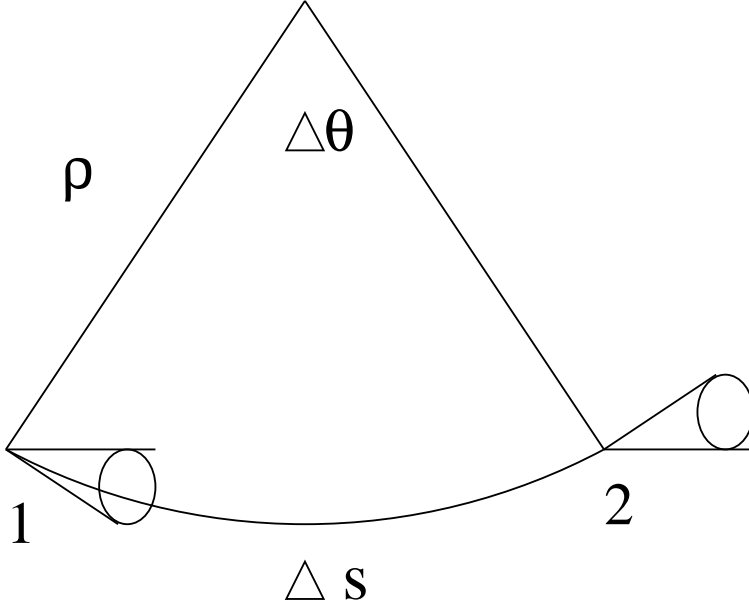
21

Figure 4.1: A particle moving along an arc of curvature radius ρ.

relativistic beaming effect. We have also $\rho\Delta\theta = \Delta s$ and $v\Delta t = \Delta s$, and therefore $\Delta t = \frac{2\rho}{\gamma v}$, where Δt is the time for the particle to move from point 1 to point 2.

To link the curvature radius ρ of the gyromotion with the field strength, note that $\gamma m \frac{\Delta\vec{v}}{\Delta t} = \frac{q}{c}\vec{v}\times\vec{B}$ and $|\Delta\vec{v}| = v\Delta\theta$, and then we have

$$\rho = \frac{\Delta s}{\Delta\theta} = \frac{v\Delta t}{|\Delta\vec{v}|/v} = \frac{v^2\gamma mc}{qBv\sin\alpha} = \frac{v}{\omega_g\sin\alpha} \ . \tag{4.8}$$

At this point, the relation between the gyroradius and the curvature radius can be found, by noting that $\omega_g r_g = v\sin\alpha$, to be $r_g = \rho\sin^2\alpha$.

The time interval of the observed pulse is then

$$
\begin{aligned}
\Delta t_{ob} &= \Delta t(1 - \frac{v}{c}) \\
&= \frac{2}{\gamma\omega_g\sin\alpha}\frac{1}{2\gamma^2} \\
&= \frac{1}{\gamma^3\omega_g\sin\alpha} \ ,
\end{aligned}
\tag{4.9}
$$

22

where we have expressed Δt in terms of ω_g and taken $\beta = 1 - \frac{1}{2\gamma^2}$ for relativistic particles. The γ^3 dependence comes from the beaming effect and the kinetic Doppler effect.

Conventionally a factor of three halfs is added to the definition of the characteristic frequency for synchrotron radiation:

$$
\begin{aligned}
\omega_c &= \frac{3}{2}\gamma^3 \omega_g \sin\alpha \\
&= \frac{3}{2}\gamma^2 \frac{qB}{mc}\sin\alpha \ .
\end{aligned}
\tag{4.10}
$$

For curvature radiation, the characteristic frequency is simply

$$
\omega_c = \frac{3}{2}\gamma^3 \frac{c}{\rho} \ ,
\tag{4.11}
$$

where the speed v is approximated with the speed of light c, as in most cases of interest.

The single-electron synchrotron radiation spectrum.

The synchrotron radiation power per frequency of a single electron in the two perpendicular linear polarization states as shown in Figure 4.2 are (Rybicki & Lightman 1979, p.179)

$$
\frac{\mathrm{d}P_\perp}{\mathrm{d}\omega} = \frac{\sqrt{3}}{4\pi}\frac{q^3}{mc^2}B\sin\alpha(F(x)+G(x)) \ ,
\tag{4.12}
$$

and

$$
\frac{\mathrm{d}P_\parallel}{\mathrm{d}\omega} = \frac{\sqrt{3}}{4\pi}\frac{q^3}{mc^2}B\sin\alpha(F(x)-G(x)) \ ,
\tag{4.13}
$$

with

$$
F(x) = x\int_x^\infty K_{\frac{5}{3}}(\xi)\mathrm{d}\xi \ ,
\tag{4.14}
$$

$$
G(x) = xK_{\frac{2}{3}}(x) \ ,
\tag{4.15}
$$

and

$$
x = \frac{\omega}{\omega_c} \ ,
\tag{4.16}
$$

23

where K's are the modified Bessel functions of order $\frac{5}{3}$ and $\frac{2}{3}$ and $\parallel$ and $\perp$ are for different polarizations defined in Figure 4.2. They are parallel and perpendicular to the projection of the magnetic field on the plane of the sky. This notation is opposite to that used in Jackson (1999), which takes the plane of motion, and therefore the direction of acceleration, as the reference to define $\parallel$ and $\perp$.
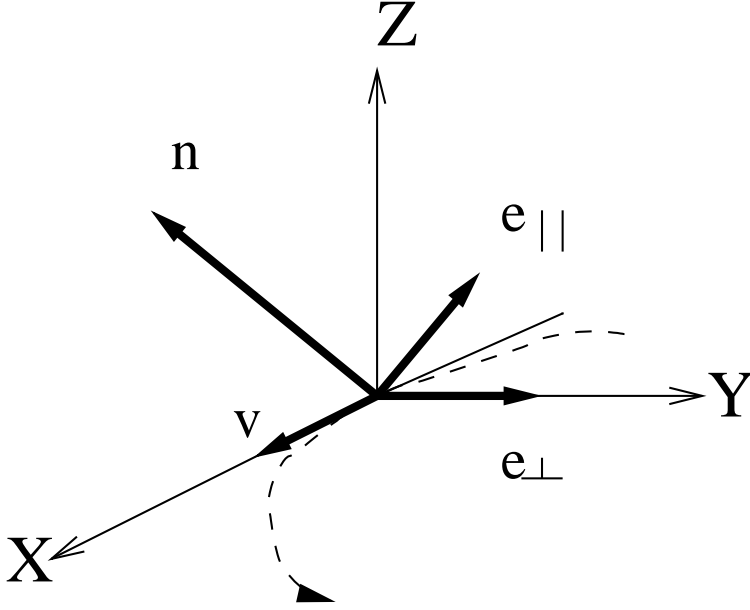

Figure 4.2: The instantaneous orbital plane is chosen to be the $X - Y$ plane with the particle velocity in the X direction. The direction towards the observer, $\hat{n}$, is chosen in the $X - Z$ plane. The directions of polarization are $\hat{e}_\perp \parallel \hat{y}$ and $\hat{e}_\parallel = \hat{n} \times \hat{e}_\perp$.

The total power spectrum is

$$\frac{\mathrm{d}P}{\mathrm{d}\omega} = \frac{\sqrt{3}}{2\pi} \frac{q^3}{mc^2} B \sin \alpha F(x) \ , \tag{4.17}$$

and

$$F(x) \sim \quad \begin{matrix} \frac{4\pi}{\sqrt{3}\Gamma(\frac{1}{3})} \left(\frac{x}{2}\right)^{\frac{1}{3}} \ , & x \ll 1 \\[2mm] \left(\frac{\pi}{2}\right)^{\frac{1}{2}} x^{\frac{1}{2}} \exp(-x) \ , & x \gg 1 \ . \end{matrix} \tag{4.18}$$

24

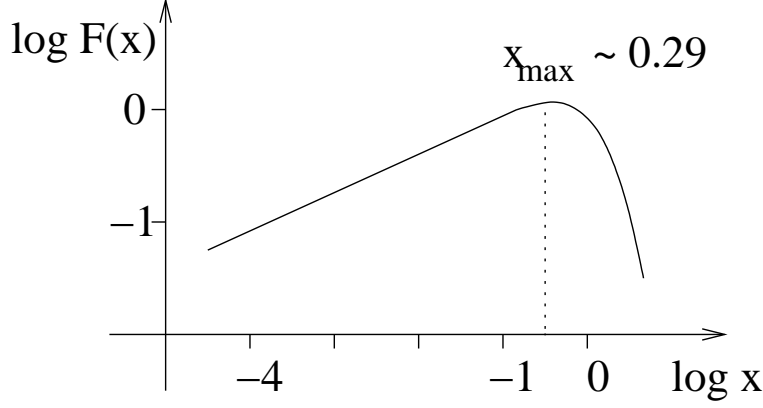The function $F(x)$ is plotted in Figure 4.3.

Figure 4.3: The synchrotron radiation spectrum of a single electron. $x = \omega/\omega_{\mathrm{c}}$.

The total emitted power.

Integrating over the frequency, we obtain the total emitted power as

$$
\begin{aligned}
P &= \int \frac{\mathrm{d}P}{\mathrm{d}\omega}\,\mathrm{d}\omega \\
&= \frac{\sqrt{3}}{2\pi}\frac{q^3}{mc^2}B\sin\alpha \int_0^\infty F(x)\mathrm{d}x(\frac{3}{2}\gamma^3\omega_{\mathrm{g}}\sin\alpha) \\
&= \frac{2}{3}\frac{q^2}{c}\gamma^2\omega_0^2\sin^2\alpha \\
&= -\dot{\gamma}_{\mathrm{syn}}mc^2
\end{aligned}
\tag{4.19}
$$

where $\int_0^\infty F(x)\mathrm{d}x = \frac{8\pi}{9\sqrt{3}}$ has been employed. We note that this is the energy loss rate via synchrotron radiation, and it depends quadratically on the particle energy γ and on the field strength B. It may be expressed in terms of the changing rate of the electron's Lorentz factor, as shown in the last equality in the above.

This result can also be obtained from the relativistic version of Larmor's formula $P = \frac{2q^2}{3c^3}\gamma^4(a_\perp^2 + \gamma^2 a_\parallel^2)$ and noting that $a_\parallel = 0$ and $a_\perp = \omega_{\mathrm{g}}v_\perp$, that is,

$$
P = \frac{2q^2}{3c^3}\gamma^4\omega_{\mathrm{g}}^2 v_\perp^2
$$

25

$$= \frac{2q^2}{3c}\gamma^2\omega_0^2\beta_\perp^2 \ . \tag{4.20}$$

We may further re-write this result in terms of Thomson cross section, $\sigma_T = \frac{8\pi}{3}(\frac{e^2}{mc^2})^2$, and the magnetic field energy density, $u_B = \frac{B^2}{8\pi}$, to get $P = 2\sigma_T c u_B \gamma^2 \beta_\perp^2$. Noting that $\beta_\perp = \beta\sin\alpha$ and $\frac{1}{4\pi}\int\sin^2\alpha\,\mathrm{d}\Omega = \frac{2}{3}$, the averaged power, for a uniform distribution in the pitch angle, is

$$\langle P\rangle_{\mathrm{syn}} = \frac{4}{3}\sigma_T c u_B \gamma^2 \beta^2 \ . \tag{4.21}$$

This should be compared with the inverse Compton energy loss rate $\dot{\gamma}_{\mathrm{ic}} mc^2 = -\frac{4}{3}\sigma_T c u_{\mathrm{ph}}\gamma^2\beta^2$ for an isotropic incident photon field discussed in the next chapter.

The curvature radiation.

With the replacement $\frac{c}{\omega_g\sin\alpha} \Rightarrow \rho$ we have the spectrum for curvature radiation:

$$\frac{\mathrm{d}P_\perp}{\mathrm{d}\omega} = \frac{\sqrt{3}}{4\pi}\frac{q^2}{\rho}\gamma(F(x)+G(x)) \tag{4.22}$$

$$\frac{\mathrm{d}P_\parallel}{\mathrm{d}\omega} = \frac{\sqrt{3}}{4\pi}\frac{q^2}{\rho}\gamma(F(x)-G(x)) \tag{4.23}$$

$$\frac{\mathrm{d}P}{\mathrm{d}\omega} = \frac{\sqrt{3}}{2\pi}\frac{q^2}{\rho}\gamma F(x) \tag{4.24}$$

The total power is

$$\begin{aligned}P &= \frac{\sqrt{3}}{2\pi}\frac{q^2}{\rho}\gamma\frac{8\pi}{9\sqrt{3}}\frac{3}{2}\gamma^3\frac{c}{\rho}\\ &= \frac{2}{3}\frac{q^2 c}{\rho^2}\gamma^4\\ &= -\dot{\gamma}_{\mathrm{cur}}mc^2 \ .\end{aligned} \tag{4.25}$$

The curvature radiation energy loss rate depends on the particle energy in the 4th power. Again, this can be obtained through $P = \frac{2q^2}{3c^3}\gamma^4(\frac{c^2}{\rho})^2$.

4.2 Synchrotron and curvature radiation of a population of electrons

The spectral index.

Consider a population of electrons with the following energy distribution:

$$N_{E,e}\mathrm{d}E = C\,E^{-p}\mathrm{d}E \ , \ E_1 < E < E_2 \ . \tag{4.26}$$

From Eq.(4.17) we have the power spectrum for a population of electrons as

$$\frac{\mathrm{d}P}{\mathrm{d}\omega} \propto \int_{\gamma_1}^{\gamma_2} F(\frac{\omega}{\omega_c})\,\gamma^{-p}\mathrm{d}\gamma \ , \tag{4.27}$$

in which the integration over energy is expressed in terms of the Lorentz factor, which enters the function F via the characteristic frequency ω_c. In this way one may derive the dependence of the power spectrum on frequency ω and obtain the spectral index of the resultant power-law spectrum.

One may also take another simpler approach by considering

$$P_\omega \mathrm{d}\omega \propto \dot{\gamma}\gamma^{-p}\mathrm{d}\gamma \ , \tag{4.28}$$

in which P_ω, as usual, is $\frac{\mathrm{d}P}{\mathrm{d}\omega}$, and a certain particle energy range $\mathrm{d}\gamma$ and its corrersponding major radiation frequency $\mathrm{d}\omega$ are considered. For synchrotron radiation, we have $\dot{\gamma} \propto \gamma^2$, $\omega \sim \omega_c \propto \gamma^2$, and $\mathrm{d}\gamma \propto \omega^{-\frac{1}{2}}\mathrm{d}\omega$, therefore

$$P_\omega \mathrm{d}\omega \propto \omega^{-\frac{p-1}{2}}\mathrm{d}\omega \ . \tag{4.29}$$

For curvature radiation, we have $\dot{\gamma} \propto \gamma^4$, $\omega \sim \omega_c \propto \gamma^3$, and $\mathrm{d}\gamma \propto \omega^{-\frac{2}{3}}\mathrm{d}\omega$. Therefore we have

$$P_\omega \mathrm{d}\omega \propto \omega^{-\frac{p-2}{3}}\mathrm{d}\omega \ . \tag{4.30}$$

The synchrotron and curvature radiation spectra of a power-law distribution of electrons with power index p are also a power law with power index $(p-1)/2$ and $(p-2)/3$ respectively. Note that the spectrum referred here is the one proportional to the flux density (F_ν), i.e., to energy flux per unit frequency. It is different from that of energy flux per decade of frequency (νF_ν) or photon number flux per unit energy $(\dot{N}_{E,\gamma} \propto F_\nu/\nu)$, which are used in different occasions.

Synchrotron radiation from a single electron in a narrow bandwidth, as observed from a certain direction, is in general elliptically polarized with its major axis perpendicular to the magnetic field direction in the sky. For a population of electrons with a smooth distribution in pitch angles, elliptical polarization will be cancelled to become partial linear polarization in the direction perpendicular to the magnetic field in the sky. The polarization degree of this linear polarization at a certain frequency (within a narrow frequency band) for a *single-energy* population is

$$\Pi(\omega) = \frac{P_{\omega,\perp} - P_{\omega,\parallel}}{P_{\omega,\perp} + P_{\omega,\parallel}} = \frac{G(x)}{F(x)} \ , \tag{4.31}$$

whose numerical value is between 0.5 and 1.
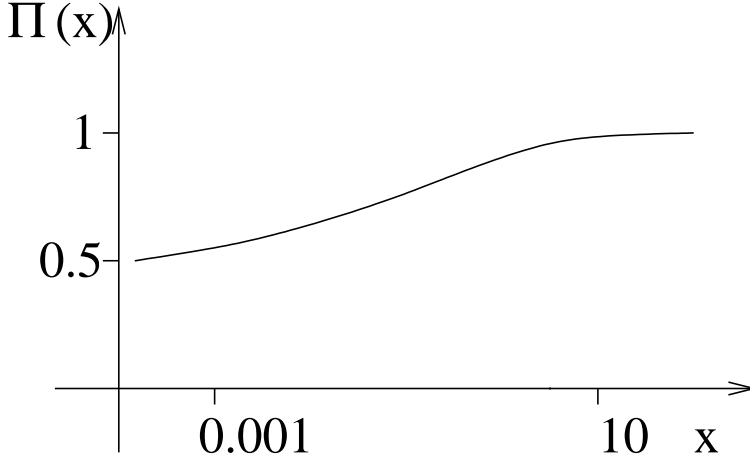

Figure 4.4: Polarization degree as a function of frequency for a single-energy population synchrotron/curvature radiation. $x = \omega/\omega_{\mathrm{c}}$.

For the radiation integrated over frequencies, noting that

$$\frac{\int_0^\infty G(x)\,\mathrm{d}x}{\int_0^\infty F(x)\,\mathrm{d}x} = \frac{3}{4} \ , \tag{4.32}$$

we therefore have

$$\Pi = \frac{P_\perp - P_\parallel}{P_\perp + P_\parallel} = 0.75 \ . \tag{4.33}$$

These results apply to both synchrotron and curvature radiation.

For a population of electrons distributed as $N_E dE = CE^{-p}dE$, we have for the synchrotron radiation

$$\Pi(\omega) = \frac{\int_0^\infty G(x)\gamma^{-p}d\gamma}{\int_0^\infty F(x)\gamma^{-p}d\gamma} \ , \tag{4.34}$$

to take into account contributions from electrons of different energy. Since $x = \omega/\omega_c$ and $\omega_c \propto \gamma^2$, we have, *for a fixed ω, $\gamma \propto (\frac{\omega}{x})^{\frac{1}{2}}$ and $d\gamma \propto \omega^{\frac{1}{2}}x^{-\frac{3}{2}}dx$.* Therefore,

$$\begin{aligned} \Pi &= \frac{\int_0^\infty G(x)\, x^{\frac{p-3}{2}}dx}{\int_0^\infty F(x)\, x^{\frac{p-3}{2}}dx} \\ &= \frac{p+1}{p+\frac{7}{3}} \ , \end{aligned} \tag{4.35}$$

which depends on the power index p but *not on the frequency ω.* This statement is probably not valid for a very large ω, since we have taken the integration over x up to infinity. By imposing $\gamma > \frac{\hbar\omega}{m_e c^2}$, we should have $x < \frac{(m_e c^2)^2}{\hbar\omega_0 \hbar\omega}$, neglecting the factors of $\frac{3}{2}$ and $\sin\alpha$. For the above result to be valid, it is required that $\frac{\hbar\omega}{m_e c^2} \ll \frac{m_e c^2}{\hbar\omega_0}$. A so-called critical field is so defined that $\hbar\omega_0 = m_e c^2$, which gives the critical field B_q as

$$B_q = 4.4 \times 10^{13}\,\mathrm{G} \ . \tag{4.36}$$

Around and above this field strength, classical electrodynamics no longer provides a good description. Way below that field strength, the validity range in ω of the above result is fairly large.

For curvature radiation, similarly, since $x = \omega/\omega_c$ and $\omega_c \propto \gamma^3$, we have, *for a fixed ω, $\gamma \propto (\frac{\omega}{x})^{\frac{1}{3}}$ and $d\gamma \propto \omega^{\frac{1}{3}}x^{-\frac{4}{3}}dx$.* Therefore,

$$\begin{aligned} \Pi &= \frac{\int_0^\infty \gamma\, G(x)\gamma^{-p}d\gamma}{\int_0^\infty \gamma\, F(x)\gamma^{-p}d\gamma} \\ &= \frac{\int_0^\infty G(x)\, x^{\frac{p-5}{3}}dx}{\int_0^\infty F(x)\, x^{\frac{p-5}{3}}dx} \\ &= \frac{p+1}{p+3} \ . \end{aligned} \tag{4.37}$$

29

One should note the γ factor in front of G and F. Consideration of the ω validity range similar to that for the synchrotron radiation gives $\frac{\hbar\omega}{m_e c^2} \ll \sqrt{\frac{m_e c^2}{\hbar(\frac{3}{2}\frac{c}{\rho})}}$.

At a first glance, it might be possible to distinguish synchrotron radiation from curvature radiation with measurement of both spectral indices and polarization degrees. However, it is unfortunate that, with a given p, the polarization degree Π is related to the spectral index α as

$$\Pi = 1 - \frac{2}{3\alpha + 5} \tag{4.38}$$

for both mechanisms. One therefore is not able to distinguish them observationally.

Some useful relations.

$$\int_0^\infty x^\mu F(x)\mathrm{d}x = \frac{2^{\mu+1}}{\mu+2}\Gamma(\frac{\mu}{2} + \frac{7}{3})\Gamma(\frac{\mu}{2} + \frac{2}{3}) \tag{4.39}$$

$$\int_0^\infty x^\mu G(x)\mathrm{d}x = 2^\mu\Gamma(\frac{\mu}{2} + \frac{4}{3})\Gamma(\frac{\mu}{2} + \frac{2}{3}) \tag{4.40}$$

$$\Gamma(n+1) = n\Gamma(n) \tag{4.41}$$
$$\Gamma(n) = (n-1)! \tag{4.42}$$
$$\Gamma(\frac{1}{2}) = \sqrt{\pi} \tag{4.43}$$
$$\Gamma(1) = 1 \tag{4.44}$$

The synchrotron self-absorption.

For synchrotron radiation, $F_\nu \propto \nu^{-\frac{p-1}{2}}$, the brightness temperature will be

$$kT_{\mathrm{b}} = \frac{c^2}{2\nu^2}\frac{F_\nu}{\Omega}$$
$$\propto \nu^{-\frac{p+3}{2}}, \tag{4.45}$$

which will be very high at low frequencies. On the other hand, self-aborption is also expected to be significant by the consideration of detailed balance.

For thermal radiation, the source function S_ν is proportional to the thermal temperature T of the system as $S_\nu \propto \nu^2 T$ for low frequencies. The brightness temperature $T_{\rm b}$ as derived from the specific intensity is always smaller than the system's thermal temperature. $T_{\rm b}$ approaches T only when the system is extremely optically thick. For non-thermal populations, although rigorous derivation may do better (Rybicki & Lightman (1979), page 189), we may take an anology by considering the source function to be $S_\nu \propto \nu^2 T_{\rm K}$, where the kinetic temperature $T_{\rm k}$ represents the particle energy, that is, $T_{\rm k} \propto \gamma$. The brightness temperature approaches $T_{\rm k}$ when the system is optically thick at low frequencies. Therefore, for such low frequencies,

$$
\begin{aligned}
F_\nu &\propto \nu^2 T_{\rm k} \\
&\propto \nu^{+\frac{5}{2}} \ ,
\end{aligned}
\tag{4.46}
$$

where in the last step we have employed $\gamma \propto \nu^{\frac{1}{2}}$ for the major frequency (characteristic frequency) being proportional to γ^2. This behavior is sketched in Figure 4.5.
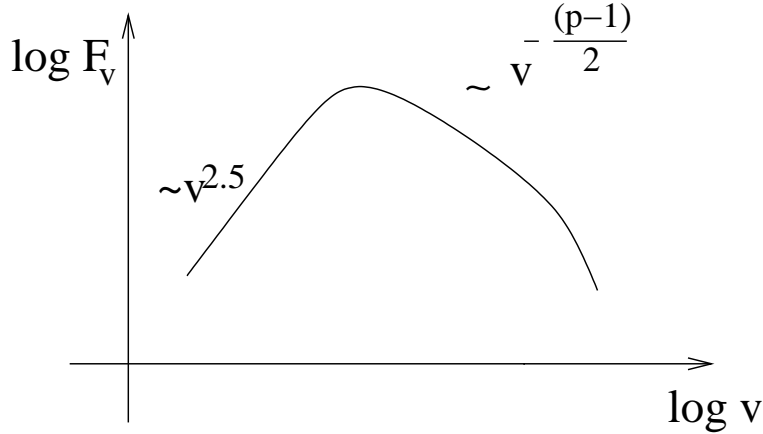

Figure 4.5: A broad-band synchrotron radiation spectrum.

31

Chapter 5

Absorption and Scattering of Photons

5.1   The interstellar photoelectric absorption

For photons of keV energy or below, absorption (i.e., photoelectric effect, bound-free absorption, photoionization) is the dominating interaction with matters. This causes considerable opacity in many systems and also in the interstellar medium. For different elements, there are different ionization energies above which the energy of photons must be so that ionization can happen. It produces some 'absorption edges' in the reaction cross section because the cross section roughly decreases as E^{-3}, where E is the photon energy. All these cross sections can be computed with quantum mechanics. For a hydrogenic electron, the cross section is (Clayton 1983, page 205; Rybicki $ Lightman 1979, page 283)

$$\sigma_{\mathrm{bf}} \propto \frac{Z^4}{\nu^3} g_{\mathrm{bf}}(\nu, Z, n, l) \;, \tag{5.1}$$

where Z is the atomic number of the element, n and l are principal and orbital quantum numbers of the original state, and ν is the photon frequency. The Gaunt factor g_{bf} has only weak dependence on its arguments. From the Z dependence we see that heavy elements play an important role. A more general compilation is shown in Figure 5.1

Photoabsorption in the interstellar medium has a non-neglible effect on soft X-rays. To have a total effective cross section for that is a complicated
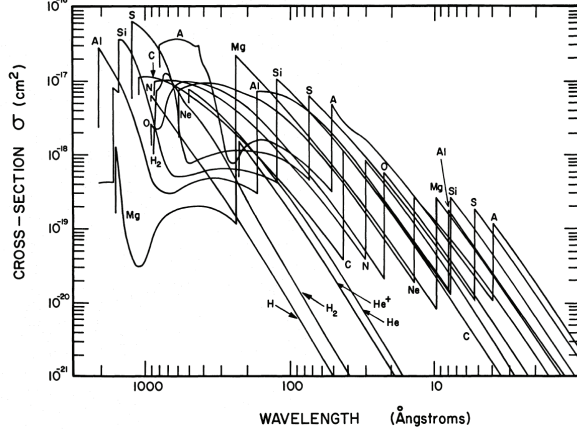
Figure 5.1: Photoabsorption cross-sections of the abundant elements in the interstellar medium (Cruddace et al. 1974).

issue. It depends on the abundance, ionization degrees and also the possibility of dusty or molecular forms. Examples of results with some specific assumptions are shown in Figure 5.2 and Figure 5.3. An approximate formula describing the corresponding optical depth is (Kembhavi & Narlikar 1999, page 279; see also Longair 2011, page 230)

$$\tau = 2.04 \left(\frac{N_{\mathrm{H}}}{10^{22}\mathrm{cm}^{-2}} \right) \left(\frac{E}{\mathrm{keV}} \right)^{-2.4} , \tag{5.2}$$

where N_{H} is the neutral hydrogen column density, which depends on local environments of the system being observed, distance, and also directions. We note that the effective cross section differs with different assumptions of cosmic abundance.

5.2 Thomson scattering

The scattering of low energy ($h\nu \ll m_{\mathrm{e}}c^2$) photons off electrons at rest can be treated with classical electrodynamics. Photons do not change energy after scattering. This is called Thomson scattering. To derive its cross section, let's review Larmor's formula first in the following. For charges of $\beta \ll 1$,
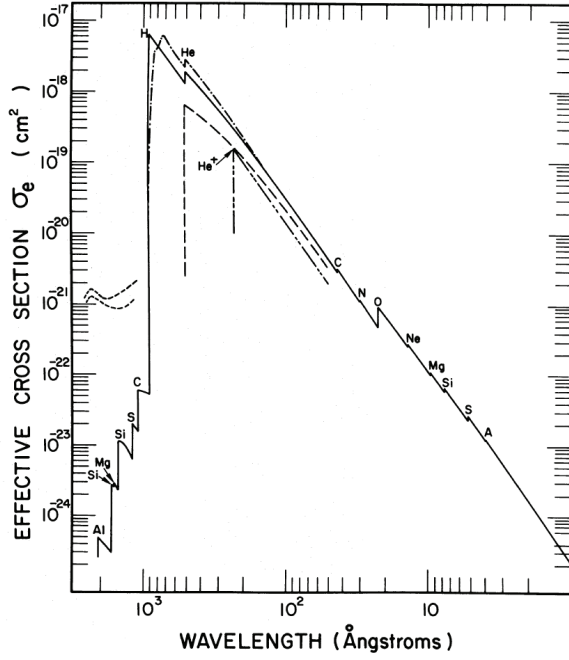
Figure 5.2: The effective photoabsorption cross-section per hydrogen atom in the interstellar medium (Cruddace et al. 1974).

the electric field of the radiation is approximately (Jackson 1975, page 658)

$$\vec{E}_{\text{rad}} = \frac{q}{c} \frac{\hat{n} \times (\hat{n} \times \dot{\vec{\beta}})}{r} \; , \tag{5.3}$$

where q is particle charge, $\hat{n}$ the unit vector in the direction of radiation propagation (i.e., towards the observer) from the charge, r the distance to the observer, and $\dot{\vec{\beta}}$ the time derivative of $\vec{\beta}$. The corresponding Pointing vector is

$$\vec{S}_{\text{rad}} = \frac{c}{4\pi} \vec{E}_{\text{rad}} \times \vec{B}_{\text{rad}} = \frac{c}{4\pi} |\vec{E}_{\text{rad}}|^2 \hat{n} \tag{5.4}$$

and the radiated power per solid angle in the direction $\hat{n}$ is

$$\frac{\mathrm{d}P}{\mathrm{d}\Omega} = r^2 |\vec{S}_{\text{rad}}| = \frac{q^2}{4\pi c} |\hat{n} \times (\hat{n} \times \dot{\vec{\beta}})|^2 \; . \tag{5.5}$$
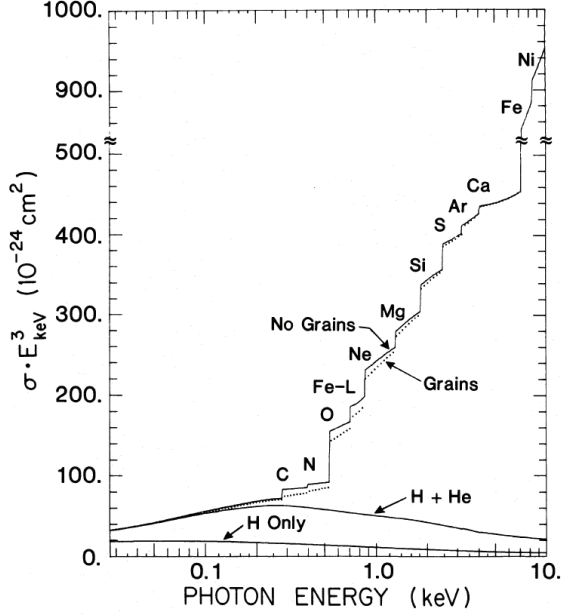
34

Figure 5.3: The effective photoabsorption cross-section per hydrogen atom in the interstellar medium (Morrison & McCammon 1983).

Let θ be the angle between $\hat{n}$ and the acceleration $\dot{\vec{v}}$. The above differential power becomes

$$\frac{\mathrm{d}P}{\mathrm{d}\Omega} = \frac{q^2}{4\pi c^3}|\dot{\vec{v}}|^2 \sin^2\theta \; . \tag{5.6}$$

From here we see the well known $\sin^2\theta$ dependence. We also note that the radiated field is polarized in the plane containing $\hat{n}$ and the acceleration $\dot{\vec{v}}$. After integrating over all solid angle, we have the total radiated power

$$P = \frac{2q^2}{3c^3}|\dot{\vec{v}}|^2 \; , \tag{5.7}$$

which is also known as **Larmor's formula** for a non-relativistic, accelerated charge.

Consider for the moment a *linearly polarized* incoming light with electric field $\vec{E}_{\mathrm{in}}$. We then have $\dot{\vec{v}} = \frac{q}{m}\vec{E}_{\mathrm{in}}$ and $S_{\mathrm{in}} = \frac{c}{4\pi}|\vec{E}_{\mathrm{in}}|^2$. Now the differential

35

power becomes, taking $q = -e$ and $m = m_e$,

$$\frac{\mathrm{d}P}{\mathrm{d}\Omega} = \frac{e^4}{m_e^2 c^4} S_{\text{in}} \sin^2 \theta \ . \tag{5.8}$$

The differential scattering cross section is $\frac{\mathrm{d}\sigma}{\mathrm{d}\Omega} = \frac{\mathrm{d}P}{\mathrm{d}\Omega}/S_{\text{in}}$, that is,

$$\frac{\mathrm{d}\sigma}{\mathrm{d}\Omega} = \left(\frac{e^2}{m_e c^2}\right)^2 \sin^2 \theta = r_e^2 \sin^2 \theta \ , \tag{5.9}$$

where r_e is the classical radius of electrons. This is the differential Thomson scattering cross section. To get the total cross section we integrate the differential one over all solid angle. The result is $\sigma_T = \frac{8\pi}{3} r_e^2$.

Now consider an *unpolarized* incoming light. We may decompose this light into two components of mutually perpendicular, linearly polarized lights. We may further choose $\hat{e}_1$ in the plane of $\hat{n}$ and $\hat{k}$, where $\hat{e}_1$ is the direction of the polarization of one incoming light component and $\hat{k}$ is the propagation direction, and choose $\hat{e}_2 = \hat{k} \times \hat{e}_1$; see Figure 5.4. Therefore the differential

Figure 5.4: $\hat{n}$ is in the plane of $\hat{e}_1$ and $\hat{k}$.

cross section is

$$\frac{\mathrm{d}\sigma}{\mathrm{d}\Omega} = \frac{1}{2}\left(\frac{\mathrm{d}\sigma}{\mathrm{d}\Omega}(\theta) + \frac{\mathrm{d}\sigma}{\mathrm{d}\Omega}(\frac{\pi}{2})\right) \tag{5.10}$$

$$= \frac{r_e^2}{2}(\cos^2 \alpha + 1) \ , \tag{5.11}$$

where the right-hand side is taken from the polarized cross section and α is the scattering angle, i.e., the angle between incoming and outgoing light, $\cos\alpha = \hat{n} \cdot \hat{k}$, as shown in Figure 5.4. The total cross section is then

$$
\begin{aligned}
\sigma_{\mathrm{T}} &= 2\pi \int \frac{\mathrm{d}\sigma}{\mathrm{d}\Omega} \mathrm{d}(\cos\alpha) \\
&= \pi r_{\mathrm{e}}^2 \int_{-1}^{1} (\cos^2\alpha + 1)\mathrm{d}(\cos\alpha) \\
&= \frac{8\pi}{3} r_{\mathrm{e}}^2 .
\end{aligned}
\tag{5.12}
$$

From the above discussion, we see that the total cross section for Thomson scattering, no matter incoming light being polarized or not, is

$$
\sigma_{\mathrm{T}} = \frac{8\pi}{3} r_{\mathrm{e}}^2 = 0.665 \times 10^{-24} \mathrm{cm}^2 .
\tag{5.13}
$$

This cross section is called the **Thomson cross section**. It is very often used to estimate the magnitude of interaction between light and matter.

A polarized light after Thomson scattering still keeps its polarization state. For unpolarized incoming light, the scattered light is in general partially linearly polarized. Recall the $\sin^2\theta$ dependence and consider contributions from the two decomposed components. We can see the polarization degree will be

$$
\Pi = \frac{1 - \cos^2\alpha}{1 + \cos^2\alpha} .
\tag{5.14}
$$

The polarization is in the direction perpendicular to the plane of $\hat{n}$ and $\hat{k}$. The polarization degree Π approaches 100% when α approaches 90°, i.e., perpendicular scattering.

5.3 Compton scattering

When the incident photon energy is comparable to the electron rest energy, the discussion of Thomson scattering is no longer valid because of the quantum nature of photons. For an electron at rest, the change of the photon energy after scattering is described as the following:

$$
\frac{\varepsilon_1}{\varepsilon} = \frac{1}{1 + \varepsilon(1 - \cos\alpha)} ,
\tag{5.15}
$$

where ε is the incident photon energy normalized by the electron rest energy, i.e., $\varepsilon = \frac{h\nu}{m_e c^2}$, ε_1 is that of the scattered photon, and α is the scattering angle. This can be re-arranged to be

$$\cos\alpha = 1 + \frac{1}{\varepsilon} - \frac{1}{\varepsilon_1} \ . \tag{5.16}$$

It can also be expressed in terms of wavelengths as

$$\frac{\Delta\lambda}{\lambda} = \frac{\lambda_1 - \lambda}{\lambda} = \varepsilon(1 - \cos\alpha) \ . \tag{5.17}$$

It shows that the fractional change in wavelength is of the order of ε. The above equation can also be arranged to be

$$\Delta\lambda = \frac{h}{m_e c}(1 - \cos\alpha) \ , \tag{5.18}$$

and the factor $\frac{h}{m_e c}$ is called the Compton wavelength of the electron.

For *unpolarized* incident photons, the cross section of the scattering is the **Klein-Nishina cross section** (Heitler 1954):

$$\frac{d\sigma}{d\Omega} = \frac{r_e^2}{2}\frac{\varepsilon_1^2}{\varepsilon^2}\left(\frac{\varepsilon}{\varepsilon_1} + \frac{\varepsilon_1}{\varepsilon} - \sin^2\alpha\right) \ . \tag{5.19}$$

We note that there is also α dependence in $\varepsilon/\varepsilon_1$. This differential cross section is always smaller than that of the Thomson scattering, to which it approaches when $\varepsilon_1 \sim \varepsilon$; see Fig. 5.5.

The total cross section can be found to be

$$\sigma_{\mathrm{KN}} = \pi r_e^2 \frac{1}{\varepsilon}\left((1 - \frac{2(\varepsilon+1)}{\varepsilon^2})\ln(2\varepsilon + 1) + \frac{1}{2} + \frac{4}{\varepsilon} - \frac{1}{2(2\varepsilon+1)^2}\right) . \tag{5.20}$$

For $\varepsilon \ll 1$,

$$\sigma_{\mathrm{KN}} \sim \frac{8}{3}\pi r_e^2(1 - 2\varepsilon) = \sigma_{\mathrm{T}}(1 - 2\varepsilon) \tag{5.21}$$

and for $\varepsilon \gg 1$,

$$\sigma_{\mathrm{KN}} \sim \pi r_e^2 \frac{1}{\varepsilon}(\ln(2\varepsilon) + \frac{1}{2}) \ . \tag{5.22}$$

To get the above approximation, $\ln(1 + x) \sim x - \frac{x^2}{2}$ is used for $x \ll 1$.
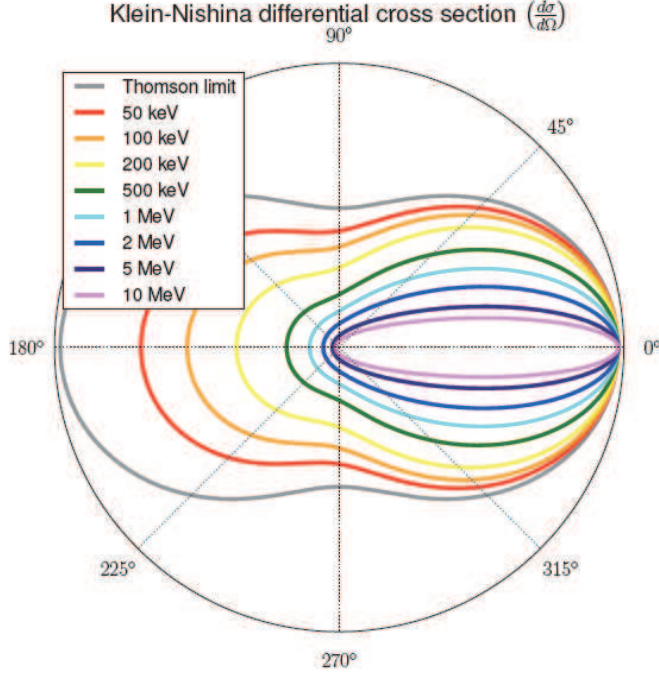
Figure 5.5: The differential Klein-Nishina cross section. (Taken from Mark Bandstra, 2010, PhD thesis, UC Berkeley)

For *polarized* incident photons,

$$\frac{d\sigma}{d\Omega} = \frac{r_e^2}{2}\frac{\varepsilon_1^2}{\varepsilon^2}\left(\frac{\varepsilon}{\varepsilon_1} + \frac{\varepsilon_1}{\varepsilon} - 2\sin^2\alpha\,\cos^2\eta\right)\;, \tag{5.23}$$

where η is the angle between the polarization of the incident photon and the scattering plane. One can see that the scattering is preferred in the direction of $\eta = \frac{\pi}{2}$ (Lei et al., 1997). This property may be employed to measure the polarization of incoming photons in Compton telescopes.

In consideration of detector designs, the recoil energy of electrons, which will be deposited in the detector and turned into electric signals, is more relevant. The electron recoil energy is

$$\begin{aligned} E_e &= m_e c^2(\varepsilon - \varepsilon_1) \\ &= m_e c^2\varepsilon\big(1 - \frac{1}{1 + \varepsilon(1 - \cos\alpha)}\big)\;. \end{aligned} \tag{5.24}$$
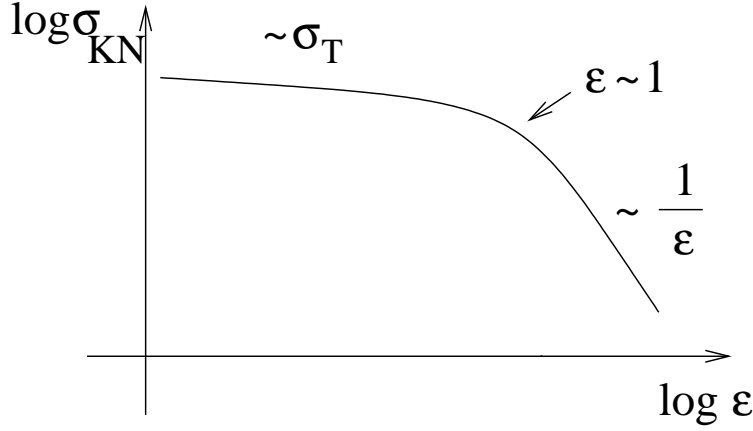
39

Figure 5.6: The Klein-Nishina cross section.

The minimum recoil energy is zero when $\alpha = 0$, and the maximum is $E_e = m_e c^2 \varepsilon \left(\frac{2\varepsilon}{1+2\varepsilon} \right)$ when $\alpha = \pi$. The gap between the incident photon energy and the maximum electron recoil energy, i.e., the energy of the back-scattered photon, is then

$$
\begin{aligned}
\varepsilon_b &= \varepsilon - E_{e,\max}/m_e c^2 \\
&= \varepsilon \left(\frac{1}{1+2\varepsilon} \right) \\
&\approx \frac{1}{2} \, ,
\end{aligned}
\tag{5.25}
$$

where the last approximation is for $2\varepsilon \gg 1$. Note that we always have $\mathrm{d}\varepsilon_b/\mathrm{d}\varepsilon > 0$, and so $\frac{1}{2}$ is the largest possible ε_b. For very high energy incident photons, $E_{e,\max}$ approaches the energy of the incident photon.

5.4 Inverse Compton scattering

If electrons are very energetic, photons after scattering tend to gain energy, instead of losing. We may take the approach similar to what is usually done for Fermi accelaration to consider the photon energy in the co-moving frame of electrons and then transform that back to the observer's frame; see Figure 5.7 and notations defined therein. Recall that a photon's energy-momentum
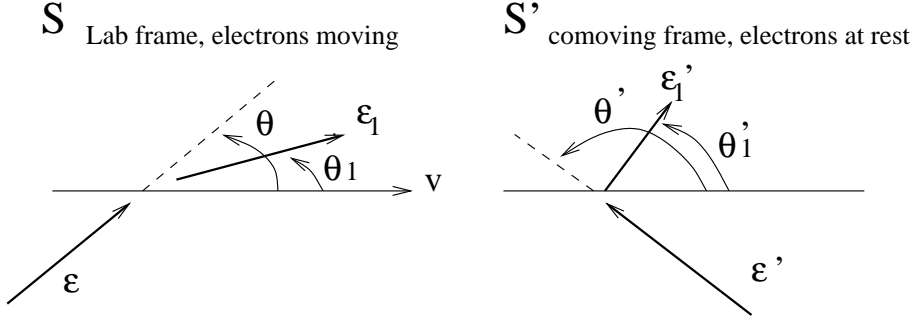
Figure 5.7: Notations used in analyzing inverse Compton scattering.

four vector is $(k_0, \vec{k})$, where $k_0 = \varepsilon/c$ and $|\vec{k}| = k_0$. It is clear that

$$\varepsilon' = \varepsilon\gamma(1 - \beta\cos\theta) \ , \tag{5.26}$$

$$\varepsilon_1' = \varepsilon'\frac{1}{1 + \varepsilon'(1 - \cos\alpha')} \ , \tag{5.27}$$

and

$$\varepsilon_1 = \varepsilon_1'\gamma(1 + \beta\cos\theta_1') \ , \tag{5.28}$$

therefore

$$\varepsilon_1 = \frac{\varepsilon\gamma^2(1 - \beta\cos\theta)(1 + \beta\cos\theta_1')}{1 + \varepsilon\gamma(1 - \beta\cos\theta)(1 - \cos\alpha')} \ . \tag{5.29}$$

We then have

$$\varepsilon_1 \sim \gamma^2\varepsilon \ , \ \text{for } \varepsilon\gamma \ll 1 \ . \tag{5.30}$$

The photon energy is boosted by a factor of γ^2. The highest energy that a photon can reach in this regime is $\varepsilon_1 = 4\gamma^2\varepsilon$ for the case of head-on collision ($\theta = \pi$, $\theta_1' = 0$). On the other hand,

$$\varepsilon_1 \sim \gamma \ \ , \ \text{for } \varepsilon\gamma \gg 1 \ . \tag{5.31}$$

In such a case electrons give almost all the energy to photons. But note that it is also possible that, when $\varepsilon > \gamma$, photons in fact give energy to electrons. The scattering cross section for $\varepsilon\gamma \gg 1$ is smaller than that for $\varepsilon\gamma \ll 1$.

41

The inverse-Compton emitted power

We now consider an electron colliding with a distribution of photons to lose energy via inverse Compton scattering. To derive the emitted power, one may in principle consider the emitted spectrum and integrate that over all frequencies. That may, however, depend on the specific distribution of the photon bath. Instead, in the following we take another approach to obtain a more general result. Let f be the phase space distribution function of photons, that is, $\mathrm{d}N = f\mathrm{d}^3p\mathrm{d}^3x$, which is a Lorentz invariant (because phase space volume is invarint; see Rybicki & Lightman 1979, p.145). The differential number density of photons at a certain energy ε is then

$$\mathrm{d}n = f\mathrm{d}^3p = g_\varepsilon\mathrm{d}\varepsilon \ . \tag{5.32}$$

Since $\mathrm{d}n/\varepsilon$ is invariant (Blumenthal & Gould 1970; see also the notes below), we have

$$\frac{g_\varepsilon\mathrm{d}\varepsilon}{\varepsilon} = \frac{g'_\varepsilon\mathrm{d}\varepsilon'}{\varepsilon'} \tag{5.33}$$

for the ambient photon field as described in different inertial frames.

The total power emitted by an electron in its rest frame is

$$\frac{\mathrm{d}E'_1}{\mathrm{d}t'} = c\sigma_\mathrm{T} \int \varepsilon' g'_\varepsilon\mathrm{d}\varepsilon' \ , \tag{5.34}$$

where we have restricted ourselves to the case of $\varepsilon\gamma \ll 1$ so that the Thomson cross section can be used and the energy change in the electron's rest frame is also neglected, i.e., that $\varepsilon'_1 = \varepsilon'$ has been adopted. Note that the emitted power for a front-back symmetric radiation pattern (in the instantaneous rest frame of the radiating particle) is Lorentz invariant (Rybicki & Lightman 1979, p.139). We then have

$$\begin{aligned}
\frac{\mathrm{d}E_1}{\mathrm{d}t} &= c\sigma_\mathrm{T} \int \varepsilon'^2 \frac{g'_\varepsilon\mathrm{d}\varepsilon'}{\varepsilon'} \\
&= c\sigma_\mathrm{T} \int \varepsilon'^2 \frac{g_\varepsilon\mathrm{d}\varepsilon}{\varepsilon} \\
&= c\sigma_\mathrm{T}\gamma^2(1 - \beta\cos\theta)^2 \int \varepsilon g_\varepsilon\mathrm{d}\varepsilon \ .
\end{aligned} \tag{5.35}$$

The last integral is in fact the photon energy density u_ph. In this equation, θ is the angle between velocities of the electron and incident photons.

The inverse Compton energy loss rate in an isotropic distribution of photons

The average of $(1 - \beta \cos \theta)^2$ over all directions is $1 + \frac{1}{3}\beta^2$. We therefore have

$$\frac{\mathrm{d}E_1}{\mathrm{d}t} = c\sigma_\mathrm{T}\gamma^2(1 + \frac{1}{3}\beta^2)u_\mathrm{ph} \tag{5.36}$$

For the energy loss rate of electrons, we should take into account the original energy carried by the incident photons per unit time, which is simply $c\sigma_\mathrm{T}u_\mathrm{ph}$. So, the energy loss rate is

$$\begin{aligned} P_\mathrm{ic} &= c\sigma_\mathrm{T}(\gamma^2(1 + \frac{1}{3}\beta^2) - 1)u_\mathrm{ph} \\ &= \frac{4}{3}\sigma_\mathrm{T}c\gamma^2\beta^2 u_\mathrm{ph} \ . \end{aligned} \tag{5.37}$$

This should be compared with P_syn.

The above discussion is good in the Thomson limit, that is, for the case that Thomson scattering is a good approximation in the electron co-moving frame, $\gamma\varepsilon \ll 1$. On the other hand, if $\varepsilon_1' < \varepsilon'$, i.e., $\varepsilon' \approx \gamma\varepsilon \geq 1$, the energy loss rate is found to be

$$P_\mathrm{ic} = \frac{4}{3}\sigma_\mathrm{T}c\gamma^2\beta^2 u_\mathrm{ph} \left(1 - \frac{63}{10}\frac{\gamma\langle\varepsilon^2\rangle}{\langle\varepsilon\rangle}\right) \ , \tag{5.38}$$

where $\langle\varepsilon^2\rangle = \int \varepsilon^2 g_\varepsilon \mathrm{d}\varepsilon$ (Blumenthal & Gould 1970). In such a case, electrons can either gain or lose energy.

Now let's consider a population of electrons. If the electrons have a certain distribution with the number density being $\mathrm{d}n_\mathrm{e} = N_{\gamma,\mathrm{e}}(\gamma)\mathrm{d}\gamma$, the total energy loss rate per unit volume is just

$$P = \int P_\mathrm{ic}N_\mathrm{e}(\gamma)\mathrm{d}\gamma \ . \tag{5.39}$$

If the electrons are in a non-relativistic thermal distribution, we have $\gamma \approx 1$, $\langle\beta^2\rangle = \langle\frac{v^2}{c^2}\rangle = \frac{3kT}{mc^2}$, and the energy loss rate per unit volume is

$$P = \left(\frac{4kT}{mc^2}\right)c\sigma_\mathrm{T}n_\mathrm{e}u_\mathrm{ph} \ . \tag{5.40}$$

This equation says that, averagely speaking, the ratio of electron's energy loss to the incident photon energy is $\left(\frac{4kT}{mc^2}\right)$. This is only valid for photons with energy smaller than kT, because we have neglected possible energy gain of electrons when making the assumption that $\varepsilon_1' = \varepsilon'$.

The inverse Compton scattering spectrum

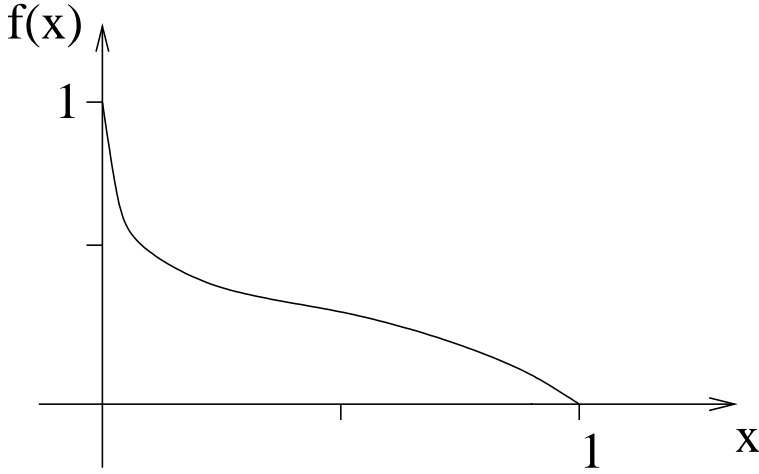
Figure 5.8: The function $f(x)$ in the single electron inverse Compton spectrum.

For an isotropic, monochromatic incident photon field at energy ε and number density n_{ph} scattered off an electron of $\gamma \gg 1$ in the Thomson limit ($\gamma\varepsilon \ll 1$), the inverse Compton scattering spectrum (energy per unit time per unit energy) is

$$\frac{\mathrm{d}P}{\mathrm{d}\varepsilon_1} = 3\sigma_{\text{T}} c n_{\text{ph}} x f(x) \ , \tag{5.41}$$

in which $x = \frac{\varepsilon_1}{4\gamma^2\varepsilon}$ and $f(x) = 2x\ln x + x + 1 - 2x^2$ (Blumenthal & Gould 1970; Note that $\frac{\mathrm{d}P}{\mathrm{d}\varepsilon_1}$ is equal to $j(\varepsilon_1) \times \frac{\varepsilon_1}{N}$ in Eq.(7.26a) of Rybicki & Lightman (1979)). The function $f(x)$ and the inverse Compton scattering spectrum of a single electron in an isotropic single-energy photon field are plotted in Figures 5.8 and 5.9, respectively.
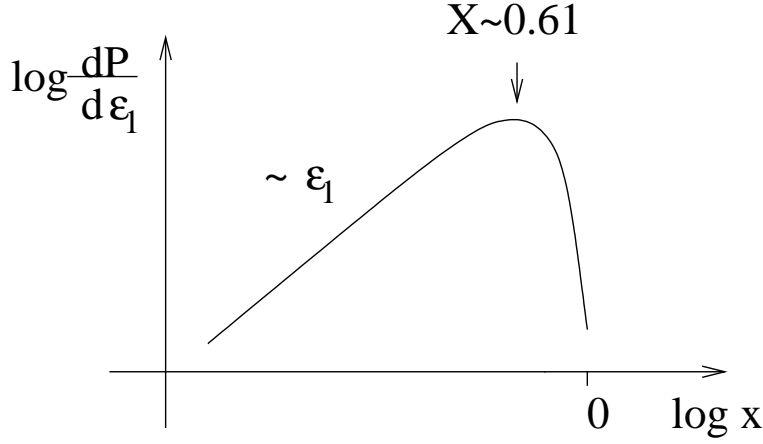
Figure 5.9: The single electron inverse Compton spectrum.

For a distribution of photons $dn_{ph} = n_{ph,\varepsilon}d\varepsilon$ scattered off electrons of a power-law distribution $dn_e \propto \gamma^{-p}d\gamma$, still isotropic and in the Thomson limit, the emissivity is

$$\frac{dP}{dVd\varepsilon_1} \propto \int n_{ph,\varepsilon}\gamma^{-p}xf(x)d\varepsilon d\gamma \ . \tag{5.42}$$

Since $x = \frac{\varepsilon_1}{4\gamma^2\varepsilon}$, we have $\gamma = \frac{1}{2}(\frac{\varepsilon_1}{\varepsilon})^{\frac{1}{2}}x^{-\frac{1}{2}}$ and $d\gamma = -\frac{1}{4}(\frac{\varepsilon_1}{\varepsilon})^{\frac{1}{2}}x^{-\frac{3}{2}}dx$ for fixed $\frac{\varepsilon_1}{\varepsilon}$.

$$\begin{aligned}
\frac{dP}{dVd\varepsilon_1} &\propto \varepsilon_1^{-\frac{p-1}{2}} \int n_{ph,\varepsilon}\varepsilon^{\frac{p-1}{2}}d\varepsilon \int_{\frac{\varepsilon_1}{4\gamma_{max}^2\varepsilon}}^{\frac{\varepsilon_1}{4\gamma_{min}^2\varepsilon}} x^{\frac{p-1}{2}}f(x)dx \\
&\propto \varepsilon_1^{-\frac{p-1}{2}} \ . \tag{5.43}
\end{aligned}$$

In the above we have assumed that the integration over x is essentially from 0 to 1 (because $\gamma_{min} \ll \gamma_{max}$) and therefore does not depend on $\varepsilon_1/\varepsilon$. The power index of this spectrum is the same as that for the synchratron radiation.

For a thermal photon field,

$$n_{ph,\varepsilon}d\varepsilon = B_\nu d\nu \times \frac{4\pi}{c\varepsilon} \ , \tag{5.44}$$

that is,

$$n_{ph,\varepsilon} = \frac{8\pi}{h^3c^3}\frac{\varepsilon^2}{\exp(\frac{\varepsilon}{kT}) - 1} \ . \tag{5.45}$$

We can see that

$$\frac{\mathrm{d}P}{\mathrm{d}V\mathrm{d}\varepsilon_1} \propto (kT)^{\frac{p+5}{2}}\varepsilon_1^{-\frac{p-1}{2}} \ , \tag{5.46}$$

that is, the emissivity depends on the photon temperature to the $\frac{p+5}{2}$ power. More detailed and more general consideration about scattering of an isotropic photon field off a population of electrons can be found in Jones (1968).

Notes to some useful Lorentz invariants

We have employed some Lorentz invariants in the above discussion. Here is a summary:

- A four-volume, i.e., a differential volume element in a four-vector space, is Lorentz invariant (Shultz 1985, p.157; Weinberg 1972, p.99).

- A phase space element, i.e., $\mathrm{d}^3x\mathrm{d}^3p$, is Lorentz invariant (Rybicki & Lightman 1979, p.145).

- The emitted power for the case of front-back symmetric radiation pattern in the rest frame of the radiating charge is invariant (Rybicki & Lightman 1979, p.139). By 'front-back symmetric' we mean for any direction of emission there is an equal probability of emission in the opposite direction. The dipole radiation adopted in Thomson scattering is such a case.

- The phase space density $\frac{\mathrm{d}N}{\mathrm{d}^3x\mathrm{d}^3p}$ is also invariant.

- The ratio of differential number density to its corresponding energy, $\mathrm{d}n/\varepsilon$, is invariant. This can be seen by noting that

$$\mathrm{d}n = \frac{\mathrm{d}N}{\mathrm{d}^3x} = \frac{\mathrm{d}N}{\mathrm{d}^4x}\mathrm{d}x_0 \ , \tag{5.47}$$

and therefore $\mathrm{d}n$ transforms like $\mathrm{d}x_0$, the time componemt of a differential displacement four-vector. Since the differential displacement four-vector is 'parallel' to its momentum four-vector ($\frac{\mathrm{d}x_i}{\mathrm{d}x_0} = \frac{p_i}{p_0}$), we

have

$$\begin{aligned}
\frac{\mathrm{d}x_0}{p_0} &= \frac{\sum \Lambda'_{0\mu}\mathrm{d}x'_\mu}{\sum \Lambda'_{0\mu}p'_\mu} \\
&= \frac{\sum \Lambda'_{0\mu}\mathrm{d}x'_\mu}{\sum \Lambda'_{0\mu}\frac{\mathrm{d}x'_\mu}{\mathrm{d}x'_0}p'_0} \\
&= \frac{\mathrm{d}x'_0}{p'_0} \ .
\end{aligned} \tag{5.48}$$

Noting that $p_0 = \varepsilon$, we then have $\mathrm{d}n/\varepsilon$ being Lorentz invariant (Blumenthal & Gould 1970).

5.5 Comptonization

The scattering between photons and electrons brings energy exchange between these two species. Very often we are interested in how the photon distribution is altered by a certain distribution of electrons through multiple scatterings. Such an action of changing the photon distribution is called Comptonization. In the following we will discuss the concept of the Compton optical depth and Comptonization in a thin medium and in a thermal medium.

The Compton y parameter (the Compton optical depth)

Let's first discuss how to parameterize the significance of Comptonization of a medium. Consider repeated scattering of low-energy photons in a finite medium. One may define a Compton y parameter as the following to describe how significantly a photon's energy is changed when it travels through the medium: $y :=$ (average fractional energy change per scattering $\Delta\varepsilon/\varepsilon$) $\times$ (average number of scattering in the medium).

For $\varepsilon \ll 1$, the energetics of Compton scattering off an electron at rest, Eq.(5.15), can be turned into

$$\frac{\varepsilon_1}{\varepsilon} = 1 - \varepsilon(1 - \cos\alpha) \ , \tag{5.49}$$

and after averaging over the scattering angle α we obtain the fractional energy change of the photon as

$$\frac{\Delta\varepsilon}{\varepsilon} = \frac{\varepsilon_1 - \varepsilon}{\varepsilon} = -\varepsilon \ . \tag{5.50}$$

When electrons are not strictly at rest, for example with thermal motions, photons may also gain energy, instead of losing. To the lowest order, we may describe the fractional energy change of photons in a single scattering with a linear combination of two small terms, ε and $kT/m_e c^2$, in the following way:

$$\frac{\Delta\varepsilon}{\varepsilon} = -\varepsilon + a\frac{kT}{m_e c^2} \ , \tag{5.51}$$

where a is a coefficient to be determined. Let's assume photons are in thermal equilibrium with electrons and the interaction between them is scattering only. In such a case photons will follow Bose-Einstein distribution with a certain chemical potential, instead of the Planck function, because the photon number is conserved. Let's further assume the number density of photons and electrons is so low that a classical description applies, i.e, photons also follow the Maxwell-Boltzmann distribution:

$$\frac{dN}{d\varepsilon} \propto \varepsilon^2 e^{-\varepsilon m_e c^2/kT} \ . \tag{5.52}$$

Noting that

$$\langle\varepsilon\rangle = \frac{\int \varepsilon \frac{dN}{d\varepsilon} d\varepsilon}{\int \frac{dN}{d\varepsilon} d\varepsilon} = \frac{3kT}{m_e c^2} \tag{5.53}$$

and

$$\langle\varepsilon^2\rangle = 12(\frac{kT}{m_e c^2})^2 \ , \tag{5.54}$$

we have

$$\begin{aligned}
\langle\Delta\varepsilon\rangle &= -\langle\varepsilon^2\rangle + a\frac{kT}{m_e c^2}\langle\varepsilon\rangle \\
&= 3(\frac{kT}{m_e c^2})^2(a - 4) \ .
\end{aligned} \tag{5.55}$$

With the requirement of $\langle \Delta \varepsilon \rangle = 0$ in equilibrium, we see that $a = 4$. Therefore, for non-relativistic electrons in thermal equilibrium, the average energy transfer per scattering is (Rybicki & Lightman 1979, p.209)

$$\frac{\Delta \varepsilon_{\mathrm{NR}}}{\varepsilon} = \frac{4kT}{m_{\mathrm{e}}c^2} - \varepsilon \; . \tag{5.56}$$

This equation describes the fractional energy change of a photon with energy ε in a thermal electron bath. The 'average' embedded is meant to be over the electron distribution. We in fact may also reach the above equation with Eq.(5.40) and Eq.(5.50). The $4kT$ term is the average fractional energy loss of a thermal electron via inverse Compton scattering when $\varepsilon \ll kT/m_{\mathrm{e}}c^2$ and $\gamma \sim 1$. The average fractional energy gain of an electron via Compton scattering is simply ε if $\varepsilon \ll 1$ and electrons are at rest. A linear combination of these two terms should still lead to the original results in limiting cases. Therefore they should be just summed together. We note that Eq.(5.56) <u>does not</u> require $\varepsilon \ll kT/m_{\mathrm{e}}c^2$. If now we further assume $\varepsilon \ll \frac{4kT}{m_{\mathrm{e}}c^2}$, we will have the average photon energy change per scattering in a thermal electronic gas to be

$$\frac{\Delta \varepsilon_{\mathrm{NR}}}{\varepsilon} = \frac{4kT}{m_{\mathrm{e}}c^2} \; . \tag{5.57}$$

For ultra-relativistic cases in the Thomson limit ($\gamma \gg 1$, $\gamma \varepsilon \ll 1$), we have

$$\frac{\Delta \varepsilon_{\mathrm{UR}}}{\varepsilon} = \frac{4}{3}\gamma^2 \; , \tag{5.58}$$

which can be obtained from Eq.(5.37). If the electrons are in thermal equilibrium, we have

$$\langle \gamma^2 \rangle = \frac{\langle E^2 \rangle}{(m_{\mathrm{e}}c^2)^2} = 12 \left(\frac{kT}{m_{\mathrm{e}}c^2} \right)^2 \; , \tag{5.59}$$

and

$$\frac{\Delta \varepsilon_{\mathrm{UR}}}{\varepsilon} \sim 16 \left(\frac{kT}{m_{\mathrm{e}}c^2} \right)^2 \; . \tag{5.60}$$

Therefore, for a thermal distribution of electrons, the Compton y parameter for non-relativistic and ultra-relativistic cases are

$$y_{\mathrm{NR}} = \frac{4kT}{m_{\mathrm{e}}c^2}\,\mathrm{Max}(\tau_{\mathrm{es}}, \tau_{\mathrm{es}}^2) \tag{5.61}$$

$$y_{\mathrm{UR}} = (\frac{4kT}{m_{\mathrm{e}}c^2})^2\,\mathrm{Max}(\tau_{\mathrm{es}}, \tau_{\mathrm{es}}^2) \ , \tag{5.62}$$

where $\tau_{\mathrm{es}} \sim \rho\kappa_{\mathrm{es}}R$, R is the dimension of the medium and $\kappa_{\mathrm{es}} = \frac{\sigma_{\mathrm{T}}}{m_{\mathrm{p}}} = 0.40$ cm^2 g^{-1}. The y-parameter is the Compton optical depth, which indicates the significance level of Comptonization in a medium.

Optically thin media: power-law spectra due to repeated scattering

When the mean amplification of photon energy per scattering is independent of the photon energy, i.e.,

$$\varepsilon_1 = A\varepsilon \ , \tag{5.63}$$

it is possible to result in a power-law emergent spectrum. Considering that $\varepsilon_1 = \varepsilon + \Delta\varepsilon = \varepsilon(1 + \frac{4}{3}\langle\gamma^2\rangle) = \varepsilon(1 + (\frac{4kT}{mc^2})^2) \approx \varepsilon(\frac{4kT}{mc^2})^2$ for an ultra-relativistic case in the Thomson limit, i.e., $\varepsilon \ll 1/\gamma$, and $\varepsilon_1 \sim \varepsilon(1 + \frac{4kT}{mc^2})$ for a non-relativistic case with $\varepsilon \ll kT/m_{\mathrm{e}}c^2$, we have A being independent of ε for both cases. The photon energy after k times scatterings is expected to be

$$\varepsilon_k \sim \varepsilon_{\mathrm{i}}A^k \tag{5.64}$$

If the medium's scattering optical depth is small, and the absorption optical depth is even much smaller, the probability for a photon to have k times scatterings before escaping from the medium is about τ_{es}^k. We therefore have

$$N(\varepsilon_k)\mathrm{d}\varepsilon_k = N(\varepsilon_{\mathrm{i}})\mathrm{d}\varepsilon_{\mathrm{i}}\tau_{\mathrm{es}}^k \ . \tag{5.65}$$

Noting that we may express τ_{es}^k in terms of $\varepsilon_k/\varepsilon_{\mathrm{i}}$ as

$$\tau_{\mathrm{es}}^k = \left(\frac{\varepsilon_k}{\varepsilon_{\mathrm{i}}}\right)^{-\mu} \ , \tag{5.66}$$

where

$$\mu = \frac{-\ln\tau_{\mathrm{es}}}{\ln A} \ , \tag{5.67}$$

and $\mathrm{d}\varepsilon_k = A^k\mathrm{d}\varepsilon_\mathrm{i} = (\varepsilon_k/\varepsilon_\mathrm{i})\mathrm{d}\varepsilon_\mathrm{i}$, we then have

$$N(\varepsilon_k) = N(\varepsilon_\mathrm{i}) \left(\frac{\varepsilon_k}{\varepsilon_\mathrm{i}}\right)^{-1-\mu} . \tag{5.68}$$

We see that a power-law spectrum can be produced by repeated scattering even when the electron distribution is not a power law. This result is similar to that in the Fermi mechanism, or shock acceleration. Note that the above is only valid for $\varepsilon_k \ll kT/m_\mathrm{e}c^2$ (NR) or $\varepsilon_k \ll m_\mathrm{e}c^2/kT$ (UR), and this is a photon number spectrum. For the photon energy spectrum (energy flux density spectrum), the power is simply $-\mu$.

Evolution of the photon spectrum in a non-relativistic thermal medium: the Kompaneets equation

A general discussion of repeated Compton scattering and the resultant spectra is complicated, when different Compton optical depth, different photon energy ranges, and other emissions from the media are involved. **The Kompaneets equation** is an equation to describe Comptonization in a non-relativistic thermal electron gas, which we will briefly discuss in the following.

The Kompaneets equation describes the evolution of photon occupation numbers. The occupation number n, or the phase space distribution function, is related to the phase space number density as

$$\frac{\mathrm{d}N}{\mathrm{d}^3x\mathrm{d}^3p} = \frac{g}{h^3} \, n \ , \tag{5.69}$$

where g is the statistical weight. For photons $g = 2$. The photon occupation number is related to the specific intensity by

$$n = \frac{I_\nu c^2}{2h\nu^3} \ , \tag{5.70}$$

where $h\nu$ is the photon energy. The above equation can be obtained with hints from the Planck function. In equilibrium, n is simply the Bose-Einstein distribution with zero chemical potential, and the relation between n and I_ν does not depend on whether it is in equilibrium or not. The assumption of isotropy is implicitly included, though. Otherwise, the specific intensity should be better replaced with the mean specific intensity. From the radiative-transfer equation and Einstein's coefficients for detailed balance

(see Eq.(1.31), Eq.(1.32) and Eq.(1.39) in the Lecture Notes for Astrophysical Radiative Processes), we have

$$\frac{\mathrm{d}n}{\mathrm{d}s} = \frac{h\nu\phi(\nu)}{4\pi}B_{21}[-n_1 n + n_2(1+n)] \ , \tag{5.71}$$

where n_1 and n_2 are number density of systems at level 1 and 2. From this example we see that the occupation number n in the term $(1+n)$ stands for stimulated processes.

The Boltzmann equation for n is, due to scatterings with a population of electrons,

$$\begin{aligned}\frac{\partial n(\omega)}{\partial t} &= c\int \mathrm{d}^3 p \int \frac{\mathrm{d}\sigma}{\mathrm{d}\Omega}\mathrm{d}\Omega(f_{\mathrm{e}}(\vec{p}_1)n(\omega_1)(1+n(\omega)) \\ &\quad -f_{\mathrm{e}}(\vec{p})n(\omega)(1+n(\omega_1)))\end{aligned} \tag{5.72}$$

where $f_{\mathrm{e}}(\vec{p})$ and $f_{\mathrm{e}}(\vec{p}_1)$ are electrons' phase space number density, ω_1 depends on $\vec{p}$ or $\vec{p}_1$ to accomplish the scattering, and $n(\omega) = n(\nu)$. The first term at the right hand side is for the increase of $n(\omega)$ due to scattering between electrons of momentum $\vec{p}_1$ and photons of frequency ω_1. The second term describes the decrease. Stimulated processes are included via n in $(1+n)$. This equation is in general difficult and complicated to solve. If the electrons are non-relativistic, the fractional energy change per scattering is small. The Boltzmann equation can be expanded to the second order in this small quantity. This approximation leads to the Fokker-Planck equation. The Fokker-Planck equation for photons scattering off a non-relativistic, thermal distribution of electrons is called the Kompaneets equation. We define the photon energy change with a dimensionless quantity Δ,

$$\Delta = \frac{\hbar(\omega_1 - \omega)}{kT} \ . \tag{5.73}$$

For the case of $\Delta \ll 1$, we can expand n to be

$$n(\omega_1) = n(\omega) + (\omega_1 - \omega)\frac{\partial n}{\partial \omega} + \frac{1}{2}(\omega_1 - \omega)^2\frac{\partial^2 n}{\partial^2 \omega} + \ldots\ldots \tag{5.74}$$

Then, the Kompaneets equation is

$$\begin{aligned}\frac{1}{c}&\frac{\partial n}{\partial t} \\ &= (n' + n(1+n))\int\int \mathrm{d}^3 p\frac{\mathrm{d}\sigma}{\mathrm{d}\Omega}\mathrm{d}\Omega f_{\mathrm{e}}\Delta \\ &\quad +(\frac{1}{2}n'' + n'(1+n) + \frac{1}{2}n(1+n))\int\int \mathrm{d}^3 p\frac{\mathrm{d}\sigma}{\mathrm{d}\Omega}\mathrm{d}\Omega f_{\mathrm{e}}\Delta^2 \ , \tag{5.75}\end{aligned}$$

52

where $n' = \partial n/\partial x$ and $x = \frac{\hbar\omega}{kT}$. This can be turned into the following form (Rybicki & Lightman 1979, p.214-215):

$$\frac{\partial n}{\partial t_{\rm c}} = \left(\frac{kT}{m_{\rm e}c^2}\right)\frac{1}{x^2}\frac{\partial}{\partial x}(x^4(n' + n + n^2)) \; , \tag{5.76}$$

with $t_{\rm c} = (n_{\rm e}\sigma_{\rm T}c)t$ is the time in units of mean time between scatterings.

Eq.(5.76) can be solved numerically in general. If the system is very optically thick, the photon spectrum reaches equilibrium after a sufficient number of scatterings. We note that the Bose-Einstein distribution ($n = (\exp(x + \alpha) - 1)^{-1}$) makes $n' + n + n^2 = 0$. On the other hand, if before reaching equilibrium, photons already escape from the system, one should include input and the escape of photons in the Kompaneets equation, that is,

$$\frac{\partial n}{\partial t_{\rm c}} = \left(\frac{kT}{mc^2}\right)\frac{1}{x^2}\frac{\partial}{\partial x}(x^4(n' + n + n^2)) + Q(x) - \frac{n}{{\rm Max}(\tau_{\rm es}, \tau_{\rm es}^2)} \; , \tag{5.77}$$

where $Q(x)$ is the source term and the escape probability per scattering is taken to be the reciprocal of the average number of scattering in the medium. Consider a steady-state solution and that Q is only non-zero for a very small x which is below the frequency range that we are concerned with. We then have

$$y_{\rm NR}\frac{\partial}{\partial x}(x^4(n' + n)) = 4nx^2 \; , \tag{5.78}$$

where the n^2 term, which is related to stimulated processes, is dropped because n is usually a very small number.

For $x \gg 1$, we may further drop nx^2, when compared with terms with x^4 in the partial derivative, and have $n' + n \approx 0$. It gives the solution that

$$n \propto e^{-x} \; , \tag{5.79}$$

which is the Wien's law: the intensity I_ν is related to the occupation number $n(\nu)$ as

$$I_\nu = \frac{2h\nu^3}{c^2}n(\nu) = \frac{2h\nu^3}{c^2}e^{-\frac{h\nu}{kT}} \; . \tag{5.80}$$

53

For $x \ll 1$, n can usually be neglected, compared with n'. Then the solution is

$$n \propto x^m ,\tag{5.81}$$

where

$$m = -\frac{3}{2} \pm \sqrt{\frac{9}{4} + \frac{4}{y_{\mathrm{NR}}}} .\tag{5.82}$$

The intensity is then

$$I_\nu \propto \nu^{3+m} .\tag{5.83}$$

The choice of the plus and minus signs in determining m is not trivial. For $y_{\mathrm{NR}} \ll 1$, the square-root term dominates. The minus sign is appropriate to avoid a positive m so that in such an optically thin case there is a simple decreasing power law to join the exponential cut off at high frequency. For $y_{\mathrm{NR}} \sim 1$ or larger, a linear combination of two power laws with different power indices should be considered. In general, when the media are more and more opaque, a thermal bump around $x \sim 1$ will appear in I_ν. An example of the computation is shown in Figure 5.10.
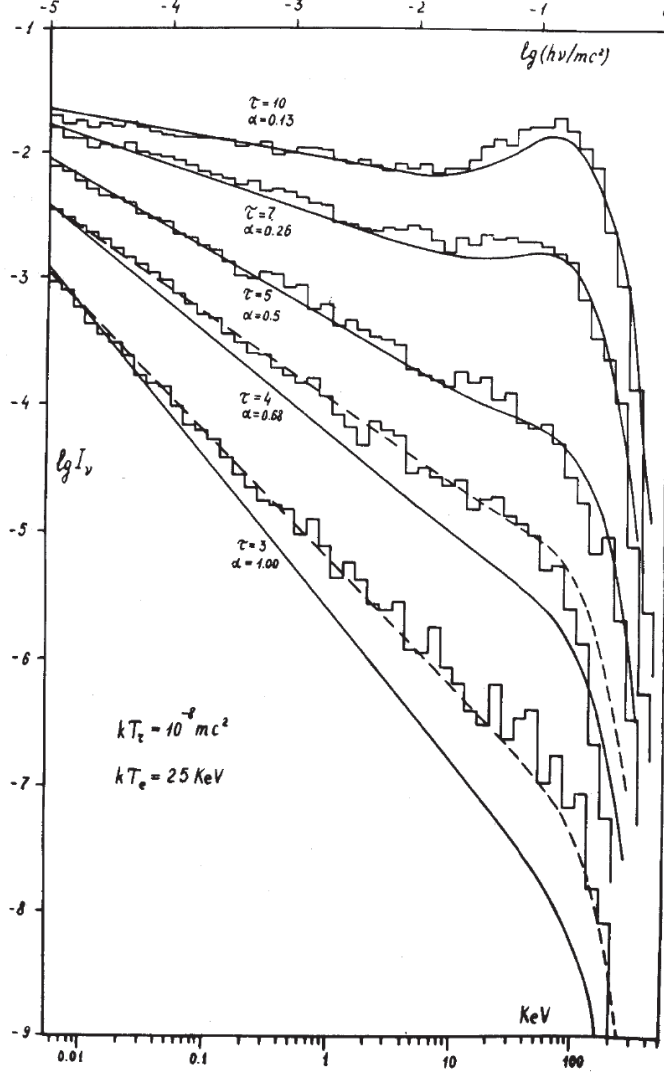
Figure 5.10: The Comptonization of low energy photons in a spherical plasma with electrons at $kT = 25$ keV (Pozdnyakov et al. 1983). Solid lines are analytic solutions, which describe the Monte Carlo simulation results (histogram) very well, except for the case of $\tau = 3$ and $\tau = 4$, for which a better fit can be obtained by assigning the spectral index α at the low energy end of the simulation to the analytic solution.

Chapter 6

Electron-Positron Pair Production

Photons can be absorbed, scattered, or converted into electron-positron pairs when they encounter matters. We have discussed absorption and scattering in the previous chapter, and now we focus on pair production. A photon cannot make pairs in free space, since in such a case energy and momentum cannot be conserved at the same time. To show this, let's consider that the best one can do to conserve energy and momentum at the same time is the case that the created electron and positron both move in the direction of the original photon propagation and share the same energy. In such a case we have, for energy conservation,

$$\hbar\omega = 2\gamma m_{\mathrm{e}}c^2$$

and for momentum conservation

$$2\gamma m_{\mathrm{e}}v = \hbar\omega/c \ .$$

It requires the speed v of the electron and positron to be equal to the speed of light c. This is not possible to achieve. Or, from the energy and momentum conservation we have

$$p_- \cos\theta_- + p_+ \cos\theta_+ = \frac{\hbar\omega}{c} = \frac{E_- + E_+}{c} \ , \tag{6.1}$$

where '$-$' and '$+$' stands for the electron and positron respectively and θ is the angle between their motion and the original photon direction. Noting

that $E^2 = p^2c^2 + m^2c^4$ one can see that the above equation is not possible to hold. Pair production of a photon can therefore only happen when there is a third body to take care of energy-momentum conservation. It can be a Coulomb field near a charge, a photon bath, or a magnetic field.

6.1 Pair production near an electric charge

The threshold energy for a photon to make pairs in a Coulomb field of a charge is $\varepsilon_{\mathrm{th}} = 2(1+\frac{m_{\mathrm{e}}}{M})$, where M is the mass of the charge (Ramana Murthy & Wolfendale 1993, page 20). When the charge is a nucleus, $M = Zm_{\mathrm{p}}$, the threshold is $\varepsilon_{\mathrm{th}} \approx 2$. When the charge is an electron, the threshold is $\varepsilon_{\mathrm{th}} = 4$. The latter is called 'triplet pair production' and is usually ignored because of its very small cross section (see, however, Mastichiadis (1991), for photons of energy larger than $250m_{\mathrm{e}}c^2$, where the triplet pair production cross section is larger than that of Compton scattering).

The cross section for photon pair production in the field of a nucleus is approximately

$$\sigma_{\gamma Z} = \alpha r_{\mathrm{e}}^2 Z^2 (\frac{28}{9}\ln(2\varepsilon) - \frac{218}{27}) \text{ for } 1 \ll \varepsilon \ll \frac{1}{\alpha Z^{1/3}} \ , \tag{6.2}$$

and

$$\sigma_{\gamma Z} = \alpha r_{\mathrm{e}}^2 Z^2 (\frac{28}{9}\ln(\frac{183}{Z^{1/3}}) - \frac{2}{27}) \text{ for } \varepsilon \gg \frac{1}{\alpha Z^{1/3}} \ . \tag{6.3}$$

One example of this cross section, together with that of absorption and scattering, is show in Figure 6.1.

The cross section is of order $\alpha r_{\mathrm{e}}^2 Z^2 = 5.8 \times 10^{-28} Z^2$ cm^2 or somewhat larger. The mean free path of a photon against pair production in the interstellar medium surely depends on the abundance and density in the ISM. Let's simply consider the interaction due to hydrogen nuclei in ISM of density 1 nucleus per cubic centimeter. The mean free path is $\ell = \frac{1}{n\sigma} \approx 5 \times 10^{26}$ cm for 10-MeV photons and $\ell \approx 10^{26}$ cm for 1-GeV photons. These are of order of 100 Mpc, not within a galaxy. Similar considertion can be applied to Compton scattering, which gives a mean free path of about 2 Mpc for 1-MeV photons. These interactions can therefore be ignored, except for regions of dense plasma.
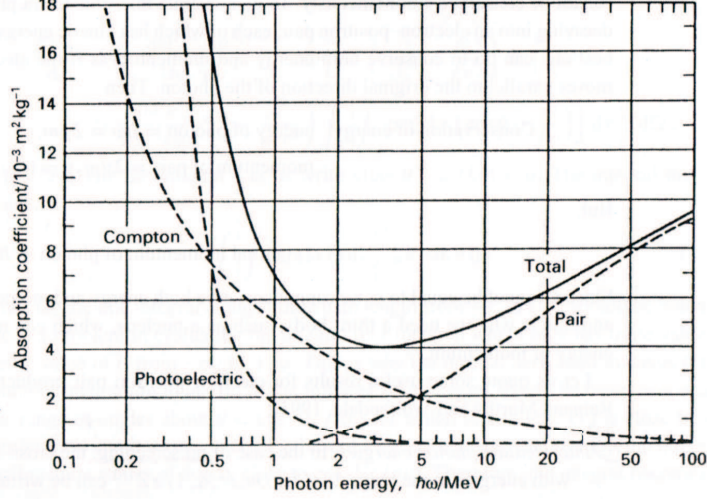
Figure 6.1: The mass absorption coefficient (opacity, $\kappa = \frac{n}{\rho}\sigma$) for photons in lead (Pb, $A = 207$, $Z = 82$, $\rho = 11.34$ g/cm^3) (Enge 1966).

In gamma-ray detectors, tungsten (W, $A = 184$, $Z = 74$, $\rho = 19.35$ g/cm^3) is often used. The mean free path for 1-GeV photons to make pairs is only about 0.4 cm. For germanium (Ge, $A = 69.7$, $Z = 32$, $\rho = 5.35$ g/cm^3), it is about 3 cm. The relative importance of photon-matter interactions is shown in Figure 6.2.

6.2 Two photon pair production

Electron-positron pairs can also be produced by photon-photon collisions. The energy threshold is

$$\varepsilon_1\varepsilon_2 > \frac{2}{1 - \cos\theta} \,, \tag{6.4}$$

where θ is the angle between the propagation directions of the two photons. For head-on collisions, we have

$$\sqrt{\varepsilon_1\varepsilon_2} > 1 \,, \tag{6.5}$$

that is, the square root of the energy product of the two photons should be larger than the rest energy of an electron, 0.511 MeV, or, the product should
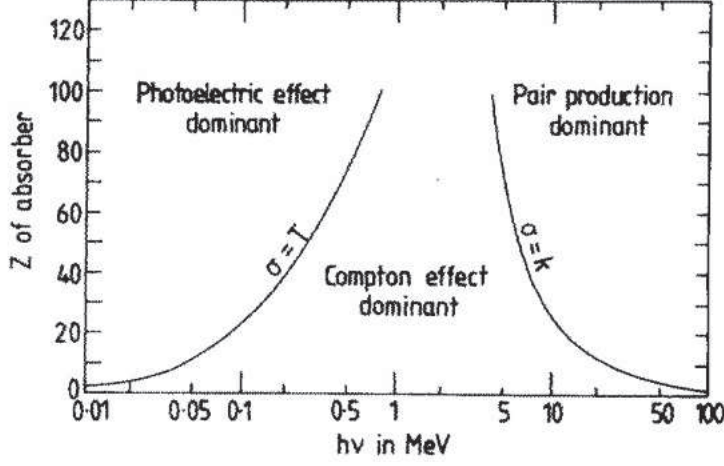
Figure 6.2: The relative importance of photon-matter interactions as a function of photon energy and the atomic number of the material involved (Evans 1955).

be larger than 0.26×10^{12} eV^2 (Longair 2011, page 276). Therefore, the threshold energy for photons colliding with CMB (6×10^{-4} eV) is about 0.4 PeV, with starlights (2 eV) about 0.1 TeV, and with X-rays (1 keV) about 0.3 GeV.

The cross section for such interaction is, for head-on collisions,

$$\sigma_{\gamma\gamma} = \pi r_{\mathrm{e}}^2 \frac{1}{\varepsilon_1 \varepsilon_2} (2 \ln(2\sqrt{\varepsilon_1 \varepsilon_2}) - 1) \text{ for } \sqrt{\varepsilon_1 \varepsilon_2} \gg 1 \; , \tag{6.6}$$

and

$$\sigma_{\gamma\gamma} = \pi r_{\mathrm{e}}^2 \sqrt{\frac{\varepsilon_1 \varepsilon_2 - 1}{\varepsilon_1 \varepsilon_2}} \text{ for } \sqrt{\varepsilon_1 \varepsilon_2} \sim 1 \; . \tag{6.7}$$

More details can be found in Jauch & Rohrlich (1976). We note that the cross section is largest for $\sqrt{\varepsilon_1 \varepsilon_2}$ being of order of unity. The mean free path of photons for two-photon pair production in CMB (photon number density about 400 cm^{-3}) is shortest (about 10 kpc) for PeV photons. At energies very close to the threshold (0.4 PeV) or as high as 10^{21} eV, it is about Gpc. See Wdowczyk et al. (1972) for more details. In systems containing an intense radiation field, two-photon pair production may be important

59

in determining the spectrum of escaping photons. In some cases, such as in the magnetosphere of gamma-ray pulsars, this mechanism also plays an important role of producing an ample flux of electrons and positrons.

6.3 One photon (magnetic) pair production

Electron-positron pairs can also be created by one photon propagating in a strong magnetic field. For a more detailed review, readers can refer to Erber (1966) and Harding (1991). Strong magnetic fields, say, stronger than 10^{12} G, are found in neutron-star systems, such as pulsars, some X-ray binaries, and isolated neutron stars in various environments. It is the major mechanism invoked in models of pulsars, both radio and high-energy ones, to produce pairs to account for their electronmagnetic emissions.

The energy threshold for one-photon pair production is

$$\varepsilon \sin \theta > 2 \ , \tag{6.8}$$

where θ is the angle between photon propagation and the magnetic field. The attenuation coefficient of one-photon pair production, $\alpha_{\gamma B}$, for photons propagating in a magnetic field of strength B is

$$\alpha_{\gamma B}(\chi) = \pi \frac{\alpha}{\lambda_{\mathrm{C}}} \frac{B_\perp}{B_{\mathrm{q}}} \mathcal{T}(\chi) = 9.36 \times 10^7 \mathrm{cm}^{-1} \frac{B_\perp}{B_{\mathrm{q}}} \mathcal{T}(\chi) \ , \tag{6.9}$$

where $\chi = \frac{\varepsilon}{2} \frac{B_\perp}{B_{\mathrm{q}}}$, α is the fine structure constant, λ_{C} the Compton wavelength of electrons, $B_\perp = B \sin \theta$, $B_{\mathrm{q}} = \frac{m_{\mathrm{e}}^2 c^3}{e\hbar} = 4.4 \times 10^{13}$ G is the critical field strength, and

$$\mathcal{T}(\chi) \approx 4.74 \chi^{-1/3} \mathrm{Ai}^2(\chi^{-2/3}) \ , \tag{6.10}$$

where Ai is the Airy function. $\mathcal{T}$ can be further approximated to be $\mathcal{T}(\chi) \approx 0.377 \exp(-\frac{4}{3\chi})$ for $\chi \ll 1$ and $\mathcal{T}(\chi) \approx 0.6\chi^{-1/3}$ for $\chi \gg 1$. The function $\mathcal{T}$ is shown in Figure 6.3.

From Eq.(6.9) we can see that even for mega-gauss fields, the attenuation length is already quite short, of order of centimeters, but this requires photons of TeV or above (to have χ of order of 10 or so). If the field strength is about $0.01 \, B_{\mathrm{q}}$, photons of GeV energy can make pairs very efficiently.
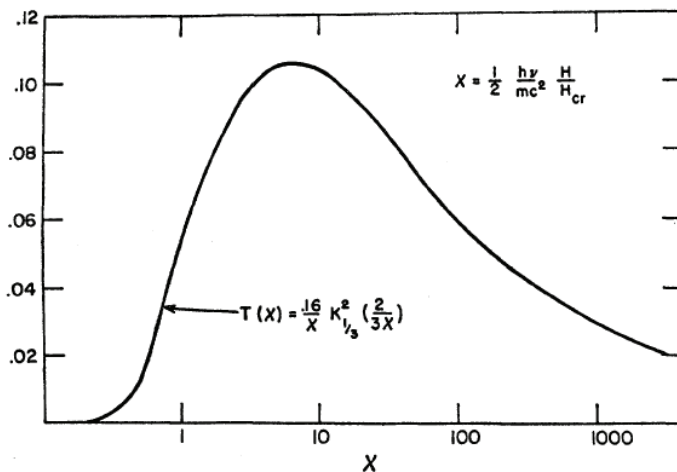
Figure 6.3: Function $\mathcal{T}$. This figure is taken from Erber (1966). Due to different conventions adopted, the $\mathcal{T}$ in this figure is a factor of 2 smaller than that in the text.

6.4 Pair-production cascade and Cherenkov radiation

When a high energy photon makes pairs, for example when it comes from outer space and hits nuclei in the upper atmosphere of the earth, these pairs may emit high energy photons through bremsstrahlung in that medium. These high energy photons may continue to make pairs and therefore a cascade develops until they are not energetic enough. When these pairs travel at a speed larger than the speed of light in that medium, i.e., $v > c/n$, where n is the refractive index of that medium (and n is frequency dependent), they emit Cherenkov radiation, which can be observed on the ground.

Discussion of the Cherenkov radiation can be found in Jackson (1975, page 639) and Longair (2011, page 264). Roughly speaking, wavefronts of the electromagnetic field variation caused by the moving charge are coherently summed in the direction of $\cos\theta = \frac{c}{nv}$, where θ is the angle between the charge motion and the radiation. The spectrum of Cherenkov radiation at

lower frequencies is, in term of specific intensity,

$$I_\omega(\omega) \propto \omega(1 - \frac{c^2}{n^2 v^2}) \; . \qquad (6.11)$$

The refractive index n is usually a complicated function of ω. The example of water as the medium is shown in Figure 6.4. For the atmosphere, very
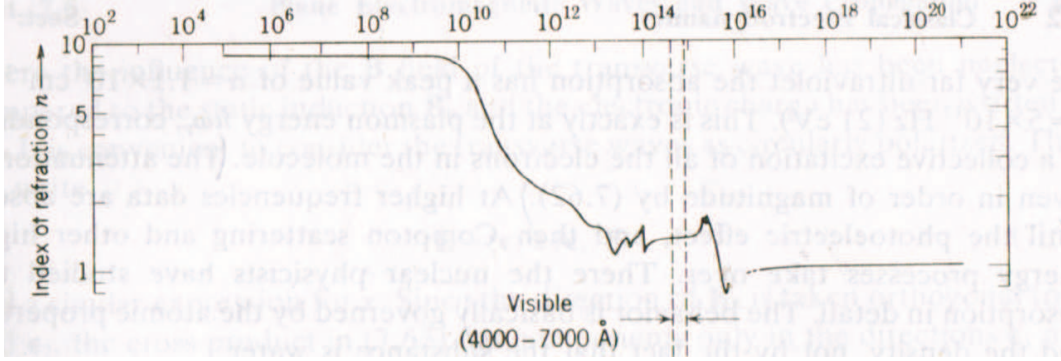

Figure 6.4: The refraction index of water. The abscissa labeled at the top is the photon frequency (Jackson 1975, page 291, Figure 7.9).

often the blue light dominates in the Cherenkov radiation.

Positrons in a cascade may annihilate with electrons in the medium, and charge asymmetry develops in the secondary charged particles. In such a case, coherent Cherenkov radiation from a bunch of charges can be emitted at longer wavelengths. This is the Askaryan effect, usually observed in microwave bands (Saltzberg et al. 2001).

6.5   Electron-positron annihilation

As touched at the end of the last section, positrons can annihilate with electrons to produce gamma-ray photons. It happens not only in a pair-production cascade, but also in other astrophysical environments where positrons are abundant. One very important example is our galactic center, from where clear, diffuse emission at 511 keV has been detected since 1970's.

Positrons may annihilate with electrons 'in flight', i.e., with relativistic energies. In such a case, most of them annihilate directly to produce two

photons. The cross section in the extreme relativistic limit is

$$\sigma = \frac{\pi r_{\mathrm{e}}^2}{\gamma}(\ln(2\gamma) - 1) \ , \tag{6.12}$$

where γ is the Lorentz factor of the positron and $r_{\mathrm{e}} = \frac{e^2}{m_{\mathrm{e}}c^2} = 2.82 \times 10^{-13}$ cm is the classical radius of electrons. The produced photons form a continuum with the highest energy being almost the energy of the original positron and the lowest at half of the electron rest energy. This cross section is, however, very small. For a 100 MeV positron, it is about 6×10^{-27} cm^2. In an ISM of $n_{\mathrm{e}} \approx 3 \times 10^{-2}$ cm^{-3}, its mean free path is about 5.6×10^{27} cm, i.e., roughly 2 Gpc. Our galaxy will be transparent to such positrons.

Positrons may lose energies through various cooling mechanisms during their travel. When their energy become lower and lower, they may be thermalized with the environment. For thermal positrons and electrons, the cross section becomes

$$\sigma \approx \frac{\pi r_{\mathrm{e}}^2}{v/c} \ , \tag{6.13}$$

and two photons at about 511 keV are produced. However, depending on the temperature, density, abundances, and ionization degrees in the environment, most of the thermal positrons may form 'positronium' with electrons (e.g. Prantzos et al. 2011) first and then annihilate. One quarter of the positronium atoms are formed in the singlet $^1S_0$ state, whose life time is 1.25×10^{-10} s. It decays into two 511-keV photons. The other three quarters are formed in the triplet $^3S_1$ state with a life time of 1.5×10^{-7} s. It decays into three photons with a maximum energy at 511 keV. These photons therefore form a continuum at the lower energy side of the 511-keV line. One example of the galactic 511-keV emission measurement and analysis can be found in Siegert et al. (2016)

Bibliography

[1] Balbus, S. A., Hawley, J. F., 1991, ApJ 376, 214

[2] Balbus, S. A., Hawley, J. F., 1998, Rev. Mod. Phys. 70, 1

[3] Becker, W., 2009 (ed), Neutron Stars and Pulsars (Springer-Verlag)

[4] Blandford, R., Eichler, D., 1987, Physics Reports 154, 1

[5] Blumenthal, G. R., Gould, R. J., 1970, Rev. Mod. Phys. 42, 237

[6] Boggs, S. E., et al., 2015, Science 348, 670

[7] Bondi, H., 1952, MNRAS 112, 195

[8] Borokowski, K. J., et al., 2010, ApJ 724, L161

[9] Chiu, H.-Y., 1968, Stellar Physics (Bleisdell Publishing Company)

[10] Churazov et al., 2014, Nature 512, 406

[11] Clayton, D. D., 1983, Principles of Stellar Evolution and Nucleosynthesis (The University of Chicago Press)

[12] Cruddace, R., et al., 1974, ApJ 187, 497

[13] Diehl, R., et al., 2006a, Nature 439, 45, 2006

[14] Diehl, R., et al., 2006b, Nuclear Physics A 777, 70

[15] Enge, H. A., 1966, Introduction to Nuclear Physics (Addison-Wesley)

[16] Erber, T., 1966, Reviews of Modern Physics 38, 626

[17] Evans, R. D., 1955, The Atomic Nucleus (McGraw-Hill)

[18] Frank, J., King, A. Raine, D. J., 2002, Accretion Power in Astrophysics, 3rd edition. Cambridge: Cambridge University Press.

[19] Goldreich, P, Julian, W. H., 1969, ApJ 157, 869

[20] Grefenstette, B. W., et al., 2014, Nature 506, 339

[21] Harding, A. K., 1991, Physics Reports 206, 327

[22] Haungs, A., et al., 2015, arXiv:1504.06696

[23] Heitler, W., 1954, The Quantum Theory of Radiation

[24] Jackson, J. D., 1975, Classical Electrodynamics, 2nd edition (John Wiley & Sons, Inc.)

[25] Jauch, J. M., Rohrlich, F., 1976, The Theory of Photons and Electrons (Springer-Verlag)

[26] Jones, F. C., 1968, Phys. Rev. 167, 1159

[27] Kembhavi, A. K., Narlikar, J. V., 1999, Quasars and Active Galactic Nuclei (Cambridge University Press)

[28] Landau, L. D., Lifshitz, E. M., 1987, Fluid Mechanics (2nd edition) (Pergamon Books Ltd.)

[29] Lei, F., et al., 1997, Space Science Reviews, 82, 309

[30] Longair, M. S., 2011, High Energy Astrophysics, 3rd edition (Cambridge University Press)

[31] Mastichiadis, A., 1991, MNRAS 253, 235

[32] Matz et al., 1988, Nature 331, 416

[33] Melia, F., 2009, High-Energy Astrophysics. New Jersey: Princeton University Press.

[34] Mihalas, D., 1978, Stellar Atmospheres, 2nd edition (W. H. Freeman and Company)

[35] Morrison, R., McCammon, D., 1983, ApJ 270, 119

[36] Narayan, R., Yi, I., 1995, ApJ 452, 710

[37] Pozdnyakov, L. A., Sobol, I. M., Sunyaev, R. A., 1983, Astrophysics and Space Physics Reviews 2, 189

[38] Prantzos, N., et al., 2011, Rev. Mod. Phys. 83, 1001

[39] Psaltis, D., 2006, in Compact Stellar X-ray Sources, ed. W. H. G. Lewin & M. van der Klis, Cambridge: Cambridge University Press. Page 1

[40] Ramaty, R., Lingenfelter, R. E., 1979, Nature 278, 127

[41] Rybicki, G. B., Lightman, A. P., 1979, Radiative Processes in Astrophysics (John Wiley & Sons, Inc.)

[42] Saltzberg, D., et al., 2001, PRL 86, 2802

[43] Shakura, N. I., Sunyaev, R. A., 1973, A&A 24, 337

[44] Siegert, T., 2016, A&A 586, A84

[45] Shultz, B. F., 1985, A First Course in General Relativity (Cambridge University Press)

[46] Wang, H., et al., 2007, A&A 469, 1005

[47] Wdowczyk, J., et al., 1972, Journal of Physics A, 5, 1419

[48] Weinberg, S., 1972, Gravitation and Cosmology (John Wiley & Sons)